

UNCLASSIFIED

~~CONFIDENTIAL~~

Copy
RM E57E14

e 2

NACA RM E57E14



RESEARCH MEMORANDUM

ANALYSIS OF LIMITATIONS IMPOSED ON ONE-SPOOL
DUCTED-FAN-ENGINE DESIGNS BY COMPRESSORS
AND TURBINES AT FLIGHT MACH NUMBERS
OF 0, 0.6, AND 0.8

By Richard H. Cavicchi

Lewis Flight Propulsion Laboratory
Cleveland, Ohio

CLASSIFICATION CHANGED

UNCLASSIFIED

LIBRARY COPY

To

By authority of

NASA + PA 9

Date

9-1-59

CLASSIFIED DOCUMENT

LIBRARY FROM

LANGLEY FIELD, VIRGINIA

NB 11-20-59

CLASSIFIED DOCUMENT

This material contains information affecting the National Defense of the United States within the meaning of the espionage laws, Title 18, U.S.C., Sec. 793 and 794, the transmission or revelation of which in any manner to an unauthorized person is prohibited by law.

NATIONAL ADVISORY COMMITTEE FOR AERONAUTICS

WASHINGTON

July 18, 1957

~~CONFIDENTIAL~~

UNCLASSIFIED

UNCLASSIFIED

NACA RM E57E14



3 1176 01436 5903

NATIONAL ADVISORY COMMITTEE FOR AERONAUTICS

RESEARCH MEMORANDUM

ANALYSIS OF LIMITATIONS IMPOSED ON ONE-SPOOL DUCTED-FAN-ENGINE

DESIGNS BY COMPRESSORS AND TURBINES AT FLIGHT MACH

NUMBERS OF 0, 0.6, AND 0.8

By Richard H. Cavicchi

SUMMARY

One-spool ducted-fan engines were analyzed at design point in order to determine the primary limitations on ducted-fan-engine design and to compare this type with the turboprop and turbojet engines for the same application. Designs were studied at flight Mach numbers of 0 and 0.6 at sea level and Mach numbers of 0.6 and 0.8 at the tropopause. High aerodynamic limits were assumed for all the turbines considered, and no allowance was made for turbine cooling. Neither burning in the bypass duct nor afterburning downstream of the turbine was considered.

The analysis revealed that the aerodynamic problems in the fan constitute a primary limitation on design for the subsonic ducted-fan engine. Turbine centrifugal stress at the rotor outlet is so low that it appears desirable to use a two-spool machine. A downstream one-stage low-speed low-stress turbine could drive the fan. The compressor could be driven by a higher-speed upstream turbine with relatively few stages in both compressor and turbine. The severity of fan aerodynamics is decreased by decreasing compressor pressure ratio, turbine-inlet temperature, and bypass ratio, and by increasing fan pressure ratio and flight Mach number.

Thrust specific fuel consumption decreases with increasing bypass ratio and increases with increasing turbine-inlet temperature and flight Mach number. Thrust per unit total weight flow decreases with increasing bypass ratio and increases with increasing turbine-inlet temperature. Mixing the bypass air with the turbine exhaust gas makes little difference in thrust specific fuel consumption and thrust per unit total weight flow. Over the range investigated, the ducted-fan engine has higher thrust specific fuel consumption and lower thrust per unit total weight flow than the turboprop engine. In both these respects, the ducted-fan engine is lower than the turbojet.

~~CONFIDENTIAL~~

UNCLASSIFIED

4507

Ug-1

INTRODUCTION

At the present time, the three main engine types being considered for flight at high subsonic Mach numbers are the turboprop, turbojet, and ducted fan. The limitations imposed on one-spool turboprop engines by compressors and turbines are analyzed in reference 1, which shows that turbine centrifugal stress at the rotor exit is high in the turboprop engine. The turbines must be designed for stresses of about 50,000 psi in order to be capable of driving high-weight-flow high-tip-speed compressors and at the same time to realize the low specific-fuel-consumption potential of turboprop engines. At turbine stresses greater than 50,000 psi, compressor aerodynamics may be a primary limitation in the turboprop engine.

Turbojet engines are similarly analyzed in reference 2. Compressor aerodynamics is a limiting factor for sea-level static conditions and for a flight condition of Mach 1.28 in the stratosphere. For flight Mach numbers of 2 and 2.8 in the stratosphere, compressor aerodynamics is relieved, but turbine centrifugal stress becomes a primary limitation.

In an effort to exploit the high aerodynamic capacity of advanced compressor design for subsonic engines, the ducted-fan engine was considered. In this type of design, a large mass of air bypasses the main compressor, the burner, and the turbine. The net result is a large, comparatively slow stream emitted from the exhaust nozzle, resulting in higher propulsive efficiency than with the turbojet engine.

This report presents a design-point analysis of one-spool ducted-fan engines designed for subsonic flight Mach numbers. The scope of the conventional cycle analysis is broadened herein by including a study of the problems of compressor aerodynamics and turbine centrifugal stress. Although this is a one-spool analysis, the results are applicable to a two-spool engine if a downstream turbine drives the fan, since in such a case the thermodynamics and the compressor and turbine parameters investigated are unaffected. The only case to which this analysis does not apply is that with a gearbox between the fan and the compressor. The object of this report is to determine the limitations imposed on ducted-fan engines by compressors and turbines and to compare this type with the turboprop and turbojet engines for the same application. This study pertains only to engines at their design point, no consideration being given to the off-design problem.

In the present analysis, engine temperature ratios from 3.0 to 6.0 and flight conditions at Mach numbers of 0 and 0.6 at sea level and 0.6 and 0.8 at the tropopause are studied. Turbine-inlet temperatures range from 1668° to 2641° R. Values from 0 to 0.8 are used for the ratio of bypass air to total incoming airflow. Compressor pressure ratios between 3 and 40 and fan pressure ratios between 1 and 3 are considered. Although

turbine-inlet temperatures up to 2641° R are analyzed, no study is made herein of the effects of turbine cooling. Neither burning in the bypass duct nor afterburning downstream of the turbine is considered.

ANALYSIS

General Considerations

The engine designs are evaluated herein in terms of turbine centrifugal stress, parameter e_F (see appendix A), thrust specific fuel consumption, and thrust per unit total weight flow.

Only turbine centrifugal stresses at the turbine rotor exit are calculated. Since temperatures are higher in the turbine first stage, it is possible that the stresses here might become a problem even though they are lower than the exit stresses. Nevertheless, the exit stress is considered a good criterion of the severity of the turbine stress problem, and it is therefore used in this report. To assess the severity of any stress problem, the existing stress must be compared with the allowable stress. Figure 1 presents a plot of the variation in rupture stress with temperature of the blade metal for M-252 metal. Curves of both 100- and 1000-hour life are shown. In order to make allowance for static and dynamic bending stresses and for thermal stresses, centrifugal stresses should not be much greater than about one-half of the values shown in figure 1.

Turbine centrifugal stresses of the order of 50,000 psi are encountered in a turboprop engine (ref. 1). The high turbine work needed to drive the propeller results in low turbine-exit temperatures. Despite these low exit temperatures, figure 1 indicates that 1000-hour life would not be achieved with 50,000-psi turbine centrifugal stress. Figure 1 does indicate, however, that the possibility of 100-hour life is marginal at this stress level if the blade metal temperature is about 1650° R. For typical values of turbine inlet and exit whirls, it can be shown that turbine relative stagnation temperature is lower than turbine-inlet temperature by approximately 60 percent of the stagnation-temperature drop across the rotor. Turbine relative stagnation temperature may be used to approximate the blade metal temperature. Thus, if turbine-inlet and exit temperatures are 2075° and 1375° R, respectively, the blade metal temperature would be approximately 1655° R. If these temperatures were to apply to the turboprop engine designed with 50,000-psi turbine centrifugal stress, 100-hour life might be possible, as previously indicated.

On the other hand, in a ducted-fan engine the stagnation-temperature drop across the turbine rotor is less. Thus, the allowable turbine centrifugal stress is lower. The lowest turbine stagnation-temperature drop, and hence the lowest allowable turbine centrifugal stress, occurs in a turbojet engine.

4307

UG-1 DAC

The significance of parameter e , discussed in references 1 and 2, will be briefly reviewed. This parameter indicates the severity of compressor aerodynamics. Parameter e is defined as

$$e = mc^2 \quad (1)$$

Low values of e are obtained from subsonic compressors, and high values from supersonic compressors. A value of 44×10^6 pounds per second³ for parameter e is currently at the fringe of multistage-compressor designs of good efficiency. For this value of e , the minimum relative Mach number $(W/a)_1$ obtainable at the compressor inlet is 1.2. Raising e while maintaining minimum $(W/a)_1$ raises the fan equivalent specific airflow m . This means that the fan diameter decreases for a given airflow. Furthermore, raising e with $(W/a)_1$ a minimum is accompanied by a rise in equivalent blade tip speed, thus requiring fewer compressor stages for a given compressor pressure ratio. This means that the compressor length decreases. Therefore, high values of e mean light and compact compressors.

If a maximum value of e_F is assigned, turbine blade centrifugal stress σ_T can be determined. If this value of σ_T is greater than the allowable stress, then σ_T limits the design. If σ_T is less than the allowable stress, then e_F limits the design. Parameter e is evaluated herein only at the fan inlet. This is the most critical point.

In this report, the term compressor pressure ratio is used to denote the ratio of stagnation pressure at the compressor outlet p_4' to that at the fan inlet p_1' .

Basis of Analysis

The foundation upon which this report is built is the relation between the parameter e_F at the fan inlet and the turbine centrifugal stress at the rotor outlet:

$$\frac{\sigma_T / \theta_1'}{e_F} = \frac{\Gamma \lambda}{288} \frac{\sqrt{518.7}}{2116} \sqrt{\frac{(k+1)R}{2kg^3}} \frac{(1+f)(1-b)}{\left(\frac{\rho V_x}{\rho' a'_{cr}}\right)_6} \sqrt{\frac{T_6' T_5'}{T_5' T_1'}} \frac{p_6'}{p_1'} \quad (B12)$$

In this equation, θ_1' is a function only of flight Mach number and altitude. The specific-weight-flow parameter $(\rho V_x / \rho' a'_{cr})_6$ is taken as constant throughout this report. The factor $(1+f)$ remains substantially

constant over the range studied in this analysis. The factors T_6'/T_5' and T_5'/T_1' are turbine and engine temperature ratios, respectively, while p_6'/p_1' is proportional to the compressor and turbine pressure ratios.

The ratio of specific heats k varies slightly from one design to another. The remaining variable in equation (B12) is the bypass ratio b ; this is the ratio of bypass air to total incoming airflow. This equation indicates that increasing b to high values greatly reduces σ_T for a given value of e_F . However, the RESULTS AND DISCUSSION section shows that turbine stress begins to increase when b reaches a value between 0.6 and 0.8.

Two variations of the ducted-fan engine are analyzed in this report. In one, the bypass air and the turbine exhaust gas are considered to expand into the atmosphere separately, unmixed (fig. 2(a)). This variation is analyzed in appendix B. In the other variation, described in appendix C and illustrated by figure 2(b), the bypass air and turbine exhaust gases are mixed before expanding into the atmosphere. The two streams are assumed to mix at the same static pressure. The charts of reference 3 were used in the mixing problem to establish the stagnation pressure after mixing. The assumptions used in this report are listed in appendix B.

Besides σ_T and e_F , two other parameters are determined in this analysis: the thrust specific fuel consumption $F(\text{sfc})$ and the thrust per unit total weight flow F/w_0 . Thrust specific fuel consumption is given by

$$F(\text{sfc}) = \frac{3600f(1-b)}{F/w_0} \quad (\text{B11})$$

for the case of nonmixing of the bypass air and turbine exhaust gas. For this case F/w_0 , as derived in appendix B, is

$$\frac{F}{w_0} = \frac{(1-b)}{g} \left[(1+f)V_7 - V_0 \right] + \frac{b}{g} (V_3 - V_0) \quad (\text{B10})$$

where V_7 is the jet velocity obtained from the turbine exhaust gas, V_3 is the jet velocity obtained from the bypass air, and V_0 denotes the free-stream velocity. In the case of mixing of the two streams, F/w_0 is derived in appendix C as

$$\frac{F}{w_0} = \frac{1}{g} \left[(1+f_9)V_{10} - V_0 \right] \quad (\text{C3})$$

where f_9 is the fuel-air ratio of the stream after mixing and V_{10} is the resulting jet velocity. For this case, thrust specific fuel consumption is

$$F(\text{sfc}) = \frac{3600gf_9}{[(1 + f_9)V_{10} - V_0]} \quad (C4)$$

All turbines in this analysis have high aerodynamic limits at the turbine exit. Thus, the turbine has the minimum exit annular area to produce the required work. A hub-tip radius ratio of 0.5 is assumed for all turbines at their exits. The flight conditions and engine temperatures studied are summarized in table I. No provision is made for the effects of cooling the turbine, as would be necessary for some of the high turbine-inlet temperatures considered. Furthermore, neither burning in the bypass duct nor afterburning downstream of the turbine is considered.

The calculations from this analysis are plotted in the form of working charts. The construction of these charts is described in appendix D. Of the many charts constructed from this analysis, only four are presented herein. These four charts are inserted at the back of the report following the figures.

RESULTS AND DISCUSSION

Discussion of Charts

Part (a) of the charts relates turbine centrifugal stress, parameter e_p , and compressor and fan pressure ratios. Parts (b) and (c) relate thrust per unit total weight flow, thrust specific fuel consumption, and compressor and fan pressure ratios for nonmixing and mixing, respectively (except for chart IV(c)). Parts (b) and (c) show the projections of surfaces on a plane. The dashed curves indicate regions behind the solid curves (or vice versa). It is important, therefore, that only intersections of solid curves with solid curves or intersections of dashed curves with dashed curves be read. Intersections of solid curves with dashed curves are imaginary and will give erroneous readings.

Chart I is constructed for sea-level static designs with a turbine-inlet temperature of 2075° R and a bypass ratio of 0.6. Minimum thrust specific fuel consumption was obtained at a compressor pressure ratio of about 20 for both nonmixing (I(b)) and mixing (I(c)). Thrust per unit weight flow is low at this value of compressor pressure ratio. Highest F/w_0 occurs at a compressor pressure ratio of about 9. For this flight condition the best fan pressure ratio is 2. A comparison of charts I(b) and (c) reveals that both lower $F(\text{sfc})$ and higher F/w_0 result with no mixing of the gas streams.

Sea-level Mach 0.6 designs at 2225° R inlet temperature show similar trends (chart II). In comparison with chart I, thrust specific fuel

consumption is considerably higher, and thrust per unit weight flow is much lower for the Mach 0.6 designs at sea level.

At the tropopause (charts III and IV) $F(\text{sfc})$ can be decreased as compressor pressure ratio is increased up to about 40 without mixing. In chart III, for Mach 0.6 designs at 2090° R inlet temperature, highest F/w_0 occurs at a compressor pressure ratio of about 12. Best fan pressure ratio is between 2.5 and 3. Nonmixing or mixing has little effect on either $F(\text{sfc})$ or F/w_0 . Comparison of charts II and III for Mach 0.6 designs shows that at the higher altitude both $F(\text{sfc})$ and F/w_0 are better than the values at sea level.

Increasing flight Mach number from 0.6 to 0.8 at the tropopause (chart IV(b)) results in higher thrust specific fuel consumption and lower thrust per unit weight flow. For this flight condition a fan pressure ratio of 2.5 yields best $F(\text{sfc})$ and F/w_0 . For all fan pressure ratios shown, a compressor pressure ratio of about 12 yields highest F/w_0 .

Chart IV(c) is a replot of chart IV(b) with the addition of curves of constant turbine centrifugal stress. These stress lines are drawn for a constant value of e_F of 44×10^6 pounds per second³. This chart shows that maximum F/w_0 would be obtained at a stress of about 12,000 psi. This occurs at a compressor pressure ratio of 11 and a fan pressure ratio of 2.5. Decreasing the fan pressure ratio while maintaining constant compressor pressure ratio lowers stress and F/w_0 and raises $F(\text{sfc})$.

Charts I to IV (and those charts not presented for the remaining turbine-inlet temperatures and bypass ratios) are crossplotted in figures 3 to 8. Several of the crossplots are constructed for a fan pressure ratio of 2, because this value generally yields good $F(\text{sfc})$ and F/w_0 . All the curves for turboprop engines that are shown in the figures were obtained from information in reference 1.

Effect of Design Parameters on Turbine Stress

Figure 3 shows the effects of compressor pressure ratio, fan pressure ratio, and bypass ratio on turbine stress for a sea-level static condition. Turbine-inlet temperature is 2075° R and parameter e_F is 44×10^6 pounds per second³. This figure shows that increasing compressor pressure ratio up to a value of about 15 for a given value of fan pressure ratio results in decreasing turbine stress. For any specified value of bypass ratio and of compressor pressure ratio, increase in fan pressure ratio results in increased turbine stress. Figure 3 shows also that increasing the bypass ratio up to 0.6 results in decreasing turbine stress. If b is further increased, the stress begins to rise, except for a fan pressure ratio of 1.5.

The findings of figure 3 are reviewed in figure 4 for the various flight Mach numbers considered. The variation in turbine stress with compressor pressure ratio, bypass ratio, and flight Mach number is shown. Turbine-inlet temperature for these four plots varies from 2075° to 2225° R; parameter e_F is 44×10^6 pounds per second³; and fan pressure ratio is 2.0. Turbine-exit temperatures are also shown as a basis for estimating the severity of turbine stress. Intersections of these curves with a bypass ratio of 0.8 are imaginary and should not be used.

The general trend of the plots in figure 4 for all flight Mach numbers considered is that turbine stress decreases with increasing compressor pressure ratio and with increasing bypass ratio (up to about 0.6 in most instances). At a compressor pressure ratio of 10 and bypass ratio of 0.6, turbine stresses are 16,500 and 17,800 psi for the sea-level static and sea-level Mach 0.6 cases, respectively (figs. 4(a) and (b)). The corresponding stresses for tropopause designs at Mach 0.6 and 0.8 are 10,500 and 10,900 psi, respectively (figs. 4(c) and (d)). Rises in flight Mach number and hence θ_1' are accompanied by rises in turbine stress in accordance with equation (B12).

In each part of figure 4 a curve for turboprop designs that represents good thrust specific fuel consumption is also shown. The curves of zero bypass ratio, of course, depict turbojet designs. In figure 4(a), a turboprop engine having the same high-tip-speed, high-weight-flow compressor as that previously mentioned for the ducted fan ($e_F = 44 \times 10^6$ lb/sec³ and $p_4/p_1 = 10$) requires a turbine designed for 49,000-psi stress compared with 16,500 psi for the ducted-fan turbine. At these two points in figure 4(a), the turbine-exit temperature is about 1400° R for the ducted fan and about 1360° R for the turboprop engine. According to the discussion in the ANALYSIS section, the blade metal temperatures are approximately 1670° and 1645° R for the ducted-fan and turboprop engines, respectively. Reference to figure 1 shows that the turbine centrifugal stress for the ducted-fan engine lies well within the 1000-hour-life limit. The turboprop design, however, is marginal for 100-hour life, where the allowable centrifugal stress is taken as one-half the stress to rupture. In the turbojet engine at a compressor pressure ratio of 10 (sea-level static, fig. 4(a)), the turbine centrifugal stress is about 26,000 psi, and the exit temperature is 1600° R. The turbojet design is thus very nearly capable of 1000-hour life.

A similar consideration at a compressor pressure ratio of 10 in figure 4(b) for sea-level Mach 0.6 designs indicates that the ducted fan would not be limited by the 1000-hour stress curve. Despite the low (1420° R) exhaust-gas temperature of the turboprop engine, the 62,000-psi centrifugal stress exceeds the 100-hour-life limit. For the turbojet engine, the 28,000-psi centrifugal stress exceeds the 100-hour-life limit because of the high (1715° R) exhaust-gas temperature.

4307

At the tropopause for both flight Mach numbers (figs. 4(c) and (d)), the turbine centrifugal stress of the ducted-fan engine is well within the 1000-hour-life limit. The turbine centrifugal stress of the turbo-prop engine again exceeds the limit given by the curve for 100-hour life. The turbojet engine is very nearly capable of 1000-hour life.

The highest centrifugal stresses occur at the flight Mach number of 0.6 at sea level, and it is for this condition that turbine-exit temperature is highest for the turboprop engine. Figure 4 shows that the ducted-fan engine is not limited by centrifugal stress except at very low compressor pressure ratios and low bypass ratios. A chart similar to chart II(b) would show that such low pressure ratios would be impractical with respect to low F/w_0 and high $F(\text{sfc})$.

Figure 4 not only reveals that turbine centrifugal stress is very low for e_F of 44×10^6 pounds per second³ but that turbine-exit temperature is also low. This indicates that it would be desirable to use a two-spool machine. With the low centrifugal stress, many stages would be required for a one-spool design. With a two-spool design, however, a low-speed low-stress downstream one-stage turbine could be used to drive the fan. Then the upstream turbine could run at higher speed and, with relatively few stages, drive the compressor, which in turn could also have relatively few stages.

A large part of the wide disparity between the turbine stress level in the ducted-fan designs and that in the turboprop designs can be attributed to the factor $(1 - b)$ in equation (B12). To explain the considerably lower value of σ_T for turbojet than for turboprop designs, it suffices to examine the factor $\sqrt{T_6'/T_5'}(p_1'/p_6')$ in equation (B12). This factor is

proportional to $(p_5'/p_6')^{1 - \frac{\eta_{\infty, T}(k-1)}{2k}}$. For ducted-fan and turbojet designs, the turbine pressure ratio p_5'/p_6' is considerably less than for turboprop designs, because for turboprop engines a high turbine pressure ratio is needed to supply the work to drive the propeller, which produces approximately 90 percent of the engine thrust. In the ducted-fan and turbojet designs, the jet produces the thrust, so that the turbine pressure ratios are lower. Since all other factors in equation (B12) are constant, assuming the same compressor pressure ratio, the parameter $(\sigma_T/\theta_1)/e_F$ is lower for the ducted-fan and turbojet engines. Thus, for a given value of e_F , turbine stress is lower for the ducted fan. Or, alternatively, as will be seen presently, for a given value of turbine stress, parameter e_F is higher for the ducted fan. These considerations of turbine stress and parameter e_F constitute a fundamental difference between the ducted-fan engine and the turboprop engine.

Figure 5 shows the effect of turbine-inlet temperature on turbine rotor-outlet centrifugal stress. Throughout figure 5, e_F is 44×10^6 pounds per second³, p_2'/p_1' is 2.0, and b is 0.6. For the ducted-fan engine, turbine stress always decreases with increasing turbine-inlet temperature. The opposite is true for turboprop engines. The turboprop curves are taken from reference 1, and they are drawn for constant values of the ratio of exhaust-nozzle area to turbine frontal area. The contrasting effects of inlet temperature on stress can be explained with the help of equation (B12). For the conditions of figure 5, σ_T is propor-

tional to $(p_5'/p_6')^{1 - \frac{\eta_{\infty, T}(k-1)}{2k}} \sqrt{\frac{T_5'}{T_1'}}$. For the turboprop curves, the charts

of reference 1 show that turbine pressure ratio remains constant if turbine-inlet temperature is increased and compressor pressure ratio and the ratio of exhaust-nozzle area to turbine frontal area remain at a fixed value. Turbine stress thus increases with rising turbine-inlet temperature T_5' for turboprop designs. For ducted-fan designs having constant b and constant fan pressure ratio p_2'/p_1' , turbine pressure ratio decreases as T_5' rises. Thus, the decrease in $(p_5'/p_6')^{1 - \frac{\eta_{\infty, T}(k-1)}{2k}}$ is greater than the increase in $\sqrt{T_5'/T_1'}$, so that turbine stress decreases as turbine-inlet temperature rises.

Effect of Design Parameters on Parameter e_F

The variation in e_F with b , T_5' , and M_0 is presented in figure 6. For these plots, compressor and fan pressure ratios are 10 and 2.0, respectively, and turbine stress is 20,000 psi. For most of the lower inlet temperatures, parameter e_F increases with increasing bypass ratio up to about 0.6 and then drops off. For the turbine-inlet temperatures of 2500° to 2600° R, e_F increases with rising b up to at least 0.8. Figure 6 also shows that, for a specified bypass ratio, increasing inlet temperature results in increasing e_F . This occurrence can be explained in the same manner as the decrease in stress with increase in turbine-inlet temperature shown in figure 5, in which e_F is held constant. At either sea level or at the tropopause, increasing flight Mach number results in decreasing e_F . This is in accordance with the variation in θ_1' .

The most important effect shown by figure 6 is the high magnitudes of parameter e_F . Except for the sea-level Mach 0.6 condition, the fringe value for e_F of 44×10^6 pound per second³ is exceeded over most of the

range of bypass ratios shown. In most cases e_F becomes prohibitively high. Meanwhile, the dotted lines show that, if the centrifugal stress in a turbine is 20,000 psi in a turboprop engine, the turbine can drive a compressor designed for a parameter e_F of well below 20×10^6 pounds per second³. The fact remains, however, that the turboprop engine can withstand much more than 20,000 psi. The values of e_F for the ducted fan are too high because of compressor aerodynamic limitations, and those for the turboprop are so low that the compressor would be too large. The difference in parameter e_F obtainable in a ducted-fan engine from that in a turboprop engine, both with constant σ_T , can be explained in the same manner used to explain stress differences in figure 4, in which e_F is constant. For the ducted-fan engine, figure 4 shows low stress in the turbine; figure 6 shows an aerodynamic problem in the fan. This is in contrast to the turboprop engine, for which figure 4 shows a high turbine stress. In figure 6, parameter e_F for the turboprop designs is too low. This can be helped by raising turbine stress, but figure 4 has shown that the turbine stress in a turboprop engine becomes high at an acceptable value of e_F . In order to relieve the exceedingly high values of e_F for the ducted-fan engine in figure 6, the turbine stress could be dropped below 20,000 psi. This is not desirable, however, because the turbine wheel speed would become too low, thus adding size to the turbine.

Effect of Design Parameters on Thrust Specific Fuel Consumption

The variation in thrust specific fuel consumption with bypass ratio is plotted in figure 7 for the four flight Mach numbers. Both mixing and nonmixing of the bypass air and turbine exhaust gases are considered. Throughout figure 7, the minimum thrust specific fuel consumption for the corresponding bypass ratio is plotted at a compressor pressure ratio of 10.

Figure 7 shows that for all flight conditions considered, except for sea-level Mach 0.6 designs at 1668° R, thrust specific fuel consumption decreases with increasing bypass ratio. In the case excepted, the chart (not included herein) used to produce this figure shows that minimum thrust specific fuel consumption occurs at a compressor pressure ratio of 6. Thus, thrust specific fuel consumption is already on the increase for this case at a compressor pressure ratio of 10. In most cases shown in figure 7, thrust specific fuel consumption is slightly lower for the nonmixed jets, but the differences are slight. Any differences are dependent upon the assumptions made.

In all cases shown in figure 7, except for sea-level Mach 0.6 designs at 1668° R, increasing turbine-inlet temperature at constant bypass ratio results in increasing thrust specific fuel consumption. This occurs because the fuel-air ratio is higher at the higher turbine-inlet temperatures, since compressor pressure ratio and flight Mach number remain the

4307

CQ-2 back

same. However, equation (B11) shows that thrust specific fuel consumption is inversely proportional to F/w_0 in addition to being proportional to f . At the higher turbine-inlet temperatures, the turbine exhaust gas is higher in temperature, with the result that V_7 (and hence (F/w_0)) is higher. Nevertheless, the rise in f is dominating; therefore, the observed trend of thrust specific fuel consumption with T_5^i occurs. Reference 4 reports that thrust specific fuel consumption decreases with increasing turbine-inlet temperature if bypass ratio is increased simultaneously. The figures in this reference, however, show that thrust specific fuel consumption increases with increasing turbine-inlet temperature if the bypass ratio remains constant, as is also shown by figure 7.

The dashed lines in figures 7(c) and (d) for turboprop designs show that thrust specific fuel consumption decreases with increasing turbine-inlet temperature. As stated previously, turbine pressure ratio remains the same for the turboprop designs as turbine-inlet temperature increases. The increase in engine temperature ratio is then sufficiently great to offset the rise in f to produce the observed result for the turboprop engine.

At both sea level and at the tropopause, figure 7 shows that increasing thrust specific fuel consumption results from increasing Mach number. This can be explained by the higher value of V_0 at higher Mach number in equation (B4), which yields a lower value of F/w_0 . This decrease in F/w_0 is reflected in increased thrust specific fuel consumption in equation (B11).

Figure 7 shows clearly the superiority of the turboprop engine over the ducted-fan engine in thrust specific fuel consumption. The turbojet designs (zero bypass ratio) yield higher thrust specific fuel consumption than the ducted-fan designs.

Effect of Design Parameters on Thrust per Unit Total Weight Flow

Figure 8 is similar to figure 7 in all respects, except that the ordinate is thrust per unit total weight flow. In the preparation of figure 8, F/w_0 was read at the point of minimum $F(\text{sfc})$ on the appropriate chart.

For all flight conditions considered, figure 8 shows that increasing bypass ratio is accompanied by decreasing F/w_0 . This offsets to some extent the decrease in thrust specific fuel consumption obtained by raising the bypass ratio. Figures 8(a) and (b) also show that F/w_0 decreases slightly with increasing M_0 at sea level. Finally, this figure shows that F/w_0 is higher for turboprop and turbojet engines than for ducted fans. This results mainly from the high value of weight flow w_0 handled by the ducted-fan engine.

SUMMARY OF RESULTS

The following results are revealed by this design-point study of the ducted-fan engine at subsonic flight Mach numbers:

1. Turbine centrifugal stress is not limiting, whereas the aerodynamics of the fan is a primary limitation on design. These results are directly opposite to those found for the turboprop engine, for which turbine stress is a primary limitation.
2. Because of the low centrifugal stress at the rotor outlet, it appears desirable to use a two-spool machine. In such a design, a downstream one-stage low-speed low-stress turbine could drive the fan. The upstream turbine could run at higher speed and, with relatively few stages, drive the compressor, which could also have relatively few stages.
3. Increases in turbine stress or, alternatively, decreases in the severity of fan aerodynamics are brought about by decreasing compressor pressure ratio, turbine-inlet temperature, and bypass ratio, and by increasing fan pressure ratio and flight Mach number.
4. Thrust specific fuel consumption decreases with increasing bypass ratio but at the expense of decreasing thrust per unit total weight flow. Both of these parameters increase with increasing turbine-inlet temperature, and thrust specific fuel consumption increases with increasing flight Mach number.
5. Whether or not the bypass air is mixed with the turbine exhaust gas makes little difference in thrust specific fuel consumption and thrust per unit total weight flow.
6. For the range investigated, the ducted-fan engine has higher thrust specific fuel consumption and lower thrust per unit total weight flow than the turboprop engine. The ducted-fan engine is lower in both these respects than the turbojet.

Lewis Flight Propulsion Laboratory
National Advisory Committee for Aeronautics
Cleveland, Ohio, May 16, 1957

APPENDIX A

SYMBOLS

A	frontal area, sq ft
A_{an}	annular area, sq ft
a	speed of sound
a'_{cr}	critical velocity, $\sqrt{\frac{2k}{k+1}} gRT'$, ft/sec
b	bypass ratio, w_2/w_0
C_n	nozzle velocity coefficient
c	equivalent tip speed, $U_t/\sqrt{\theta'_1}$, ft/sec
e	engine parameter used in relating compressors and turbines, mc^2 , lb/sec ³
F	thrust, lb
F(sfc)	thrust specific fuel consumption, lb fuel/(lb thrust)(hr)
f	fuel-air ratio, lb fuel/lb air
g	gravitational constant, 32.17 ft/sec ²
H	lower heating value of fuel at 600° R, Btu/lb
h	specific enthalpy, Btu/lb
h_f	initial enthalpy of fuel, Btu/lb fuel
J	mechanical equivalent of heat, 778.2 ft-lb/Btu
k	ratio of specific heats for gas
M	Mach number
m	equivalent weight flow per unit frontal area, $\frac{w\sqrt{\theta'_1}}{AS'_1}$, lb/(sec)(sq ft)
p	absolute pressure, lb/sq ft

R	gas constant, 53.4 ft-lb/(lb)(°R)
r	radius, ft
T	absolute temperature, °R
U	blade velocity, ft/sec
V	absolute velocity, ft/sec
W	relative velocity, ft/sec
w	weight flow, lb/sec
Γ	density of blade metal, lb/cu ft
γ	ratio of specific heats for air
δ	ratio of pressure to NACA standard sea-level pressure of 2116 lb/sq ft
η _B	burner efficiency
η _∞	small-stage efficiency
θ	ratio of temperature to NACA standard sea-level temperature of 518.7° R
λ	stress-correction factor for tapered blades
ρ	density of gas, lb/cu ft
σ	blade centrifugal stress at hub radius, psi
ψ _h	$\frac{(h - h_a)(1 + f)}{f}$, Btu/lb

Subscripts:

a	air
C	compressor
F	fan
h	hub

T turbine

t tip

x axial component

0-10 station numbers shown in fig. 2

Superscript:

' stagnation state relative to stator

APPENDIX B

ASSUMPTIONS AND ANALYSIS FOR BYPASS AIR NOT MIXED
WITH TURBINE EXHAUST GAS

Assumptions

The following values were assumed for design variables:

$(\rho V_x / \rho' a_{cr}')_6$	0.562
$p_1'/p_0' = p_3'/p_2' = p_5'/p_4' = p_7'/p_6' = p_{10}'/p_9'$	0.95
Turbine hub-tip radius ratio, $(r_h/r_t)_6$	0.5
Compressor or fan small-stage efficiency, $\eta_{\infty,C} = \eta_{\infty,F}$	0.88
Turbine small-stage efficiency, $\eta_{\infty,T}$	0.85
Burner efficiency, η_B	0.95
Exhaust-nozzle velocity coefficient, C_n	0.96
Lower heating value of fuel, H , Btu/lb fuel	18,574
Initial fuel enthalpy, h_f , Btu/lb fuel	-50
Blade metal density, Γ , lb/cu ft	500
Ratio of specific heats for air, γ	1.4
Gravitational constant, g , ft/sec ²	32.17
Mechanical equivalent of heat, J , ft-lb/Btu	778.2
Gas constant, R , ft-lb/(lb)(°R)	53.4

Analysis

Ranges of values were assigned to engine temperature ratio, bypass ratio, and compressor and fan pressure ratios. The bypass ratio as used herein is defined as

$$b = \frac{w_2}{w_0} \tag{B1}$$

The relation among the work of turbine, compressor, and fan is

$$(1 - b)(1 + f)(h_5' - h_6') = (1 - b)(h_4' - h_1') + b(h_2' - h_1') \tag{B2}$$

in which $h_4' - h_1'$ and $h_2' - h_1'$ are obtained from the compressor and fan pressure ratios, respectively, by use of reference 5. This reference is also used to calculate turbine pressure ratio from $h_5' - h_6'$.

Fuel-air ratio f is calculated by

$$f = \frac{h_{a,5}^i - h_{a,4}^i}{\eta_B H - h_{a,5}^i - \psi_{h,5}^i + h_f} \quad (B3)$$

which is given in reference 5.

Engine thrust is

$$F = \frac{w_4}{g} \left[(1 + f)V_7 - V_0 \right] + \frac{w_2}{g} (V_3 - V_0) \quad (B4)$$

The jet velocities V_7 and V_3 are calculated by

$$V_7 = C_n \left\{ 2gR \frac{k}{k-1} T_7^i \left[1 - \left(\frac{p_0}{p_7^i} \right)^{\frac{k-1}{k}} \right] \right\}^{0.5} \quad (B5)$$

and

$$V_3 = C_n \left\{ 2gR \frac{\gamma}{\gamma-1} T_3^i \left[1 - \left(\frac{p_0}{p_3^i} \right)^{\frac{\gamma-1}{\gamma}} \right] \right\}^{0.5} \quad (B6)$$

using

$$\frac{p_0}{p_7^i} = \left(\frac{p}{p^i} \right)_0 \frac{p_0^i}{p_1^i} \frac{p_1^i}{p_4^i} \frac{p_4^i}{p_5^i} \frac{p_5^i}{p_6^i} \frac{p_6^i}{p_7^i} \quad (B7)$$

and

$$\frac{p_0}{p_3^i} = \left(\frac{p}{p^i} \right)_0 \frac{p_0^i}{p_1^i} \frac{p_1^i}{p_2^i} \frac{p_2^i}{p_3^i} \quad (B8)$$

From the definition of bypass ratio given by equation (B1),

$$w_4 = (1 - b)w_0 \quad (B9)$$

Hence, engine thrust per unit incoming total airflow is

$$\frac{F}{w_0} = \frac{(1-b)}{g} [(1+f)V_7 - V_0] + \frac{b}{g} (V_3 - V_0) \quad (B10)$$

Thrust specific fuel consumption is

$$F(\text{sfc}) = \frac{3600f(1-b)}{F/w_0} \quad (B11)$$

The turbine blade centrifugal stress and compressor parameter e_F are related by

$$\frac{\sigma_T/\theta_1}{e_F} = \frac{\Gamma \lambda}{288} \frac{\sqrt{518.7}}{2116} \sqrt{\frac{(k+1)R}{2kg^3}} \frac{(1+f)(1-b)}{\left(\frac{\rho V_x}{\rho a_{cr}}\right)_6} \sqrt{\frac{T_6^i T_5^i}{T_5^i T_1^i}} \frac{P_6^i}{P_1^i} \quad (B12)$$

Parameter e , described in references 1 and 2, is

$$e = mc^2$$

Parameters e for compressors and turbines are related by

$$e_T = (1+f)(1-b)e_C \quad (B13)$$

APPENDIX C

ANALYSIS FOR BYPASS AIR MIXED WITH TURBINE EXHAUST GAS

In the analysis for bypass air mixed with turbine exhaust gas, equations (B1) to (B3) again hold true. The continuity equation can be expressed as

$$w_0(1 + f_5)(1 - b) + w_0b = w_0(1 + f_9) \quad (C1)$$

yielding

$$f_9 = f_5(1 - b) \quad (C2)$$

Engine thrust per unit total incoming weight flow is

$$\frac{F}{w_0} = \frac{1}{g} \left[(1 + f_9)V_{10} - V_0 \right] \quad (C3)$$

Thrust specific fuel consumption is, by equations (B11), (C2), and (C3),

$$F(\text{sfc}) = \frac{3600gf_9}{[(1 + f_9)V_{10} - V_0]} \quad (C4)$$

In the mixing process between stations 8 and 9, the momentum equation yields

$$A_{an,3}p_3 + \left(\frac{w_0}{g}\right)bV_3 + A_{an,7}p_7 + \left(\frac{w_0}{g}\right)(1 - b)(1 + f_5)V_7 = \left(\frac{w_0}{g}\right)(1 + f_9)V_9 + A_{an,9}p_9 \quad (C5)$$

and the energy equation,

$$(1 - b)(1 + f_5)h_7^* + bh_3^* = (1 + f_9)h_9^* \quad (C6)$$

With

$$\frac{p_8}{p^*} > \left(\frac{2}{k_7 + 1}\right)^{\frac{k_7}{k_7 - 1}} \quad (C7)$$

4307

then

$$p_7 = p_8 = p_3 \quad (C8)$$

Station 7 is not choked. It was assumed that

$$A_{an,8} = A_{an,9} = A_{an,7} + A_{an,3}$$

For each point calculated, the Mach number in the duct was chosen as that value which resulted in highest jet velocity V_{10} . In the present analysis, the charts of reference 3 were used to solve the mixing problem. The stagnation pressure after mixing p'_9 having been thus determined, the jet velocity was calculated by

$$V_{10} = C_n \left\{ 2gR \frac{k_9}{k_9 - 1} T'_{10} \left[1 - \left(\frac{p_0}{p'_{10}} \right)^{\frac{k_9 - 1}{k_9}} \right] \right\}^{0.5} \quad (C9)$$

Equations (B12) and (B13) again apply for stress and parameter e_F .

APPENDIX D

CONSTRUCTION OF CHARTS

For each turbine-inlet temperature and flight Mach number considered, a set of charts was constructed from the calculated data. These charts follow the figures in this report. Table I summarizes the flight conditions studied in this analysis. Four charts are presented herein as representative, one for each flight Mach number and altitude considered. For these four charts the turbine-inlet temperatures are approximately 2100° to 2200° R and the ratio of bypass to total airflow is 0.6.

Part (a) of the charts relates compressor and fan pressure ratios, parameter e_F , and turbine centrifugal stress. Throughout this report, by the term "compressor pressure ratio" is meant the over-all stagnation pressure ratio from fan inlet to compressor outlet - that is, p_4'/p_1' . The left side of part (a) of the charts consists merely of straight lines, the extensions of which would pass through the origin of $\sigma_T/\theta_1 e_F$ against σ_T . The right side of part (a) is plotted directly from calculated data of $\sigma_T/\theta_1 e_F$ against p_4'/p_1' with curves of constant p_2'/p_1' .

Parts (b) and (c) of the charts relate thrust per unit total airflow, thrust specific fuel consumption, and compressor and fan pressure ratios. Part (b) pertains to the case of nonmixing of bypass air and turbine exhaust gas, and part (c) pertains to mixing. From calculated data, F/w_0 was plotted against p_4'/p_1' for lines of constant p_2'/p_1' . Similarly, $F(sfc)$ was plotted against p_4'/p_1' . These two preliminary plots were then read at selected values of compressor pressure ratio to produce parts (b) and (c) of the charts. In chart IV, no part is shown for mixing, because this particular flight condition was not analyzed in this manner.

REFERENCES

1. Cavicchi, Richard H.: Analysis of Limitations Imposed on One-Spool Turboprop-Engine Designs by Compressors and Turbines at Flight Mach Numbers of 0, 0.6, and 0.8. NACA RM E56I05, 1956.
2. Cavicchi, Richard H., and English, Robert E.: Analysis of Limitations Imposed on One-Spool Turbojet-Engine Designs by Compressors and Turbines at Flight Mach Numbers of 0, 2.0, and 2.8. NACA RM E54F21a, 1954.
3. Turner, L. Richard, Addie, Albert N., and Zimmerman, Richard H.: Charts for the Analysis of One-Dimensional Steady Compressible Flow. NACA TN 1419, 1948.
4. Collins, D. F., Martlew, D. L., and Smith, Janet L.: The Effect on the Performance of the Bypass Engine of Raising the Design Maximum Cycle Temperature. Memo. M.166, British NGTE, Dec. 1952.
5. English, Robert E., and Wachtl, William W.: Charts of Thermodynamic Properties of Air and Combustion Products from 300° to 3500° R. NACA TN 2071, 1950.

TABLE I. - SUMMARY OF FLIGHT CONDITIONS AND
ENGINE TEMPERATURES STUDIED

Altitude, ft	Flight Mach number, M_0	Flight velocity		Engine tem- pera- ture ratio, T_5^t/T_1^t	Turbine- inlet tempera- ture, T_5^t , °R	Chart
		mph	knots			
Sea level	0	0	0	4 5	2075 2593	I ---
	0.6	456	396	3 4	1668 2225	--- II
36,089	0.6	396	344	4	1672	---
				5	2090	III
				6	2509	---
0.8	528	458	4	1760	---	
			5	2200	IV	
			6	2641	---	

4307

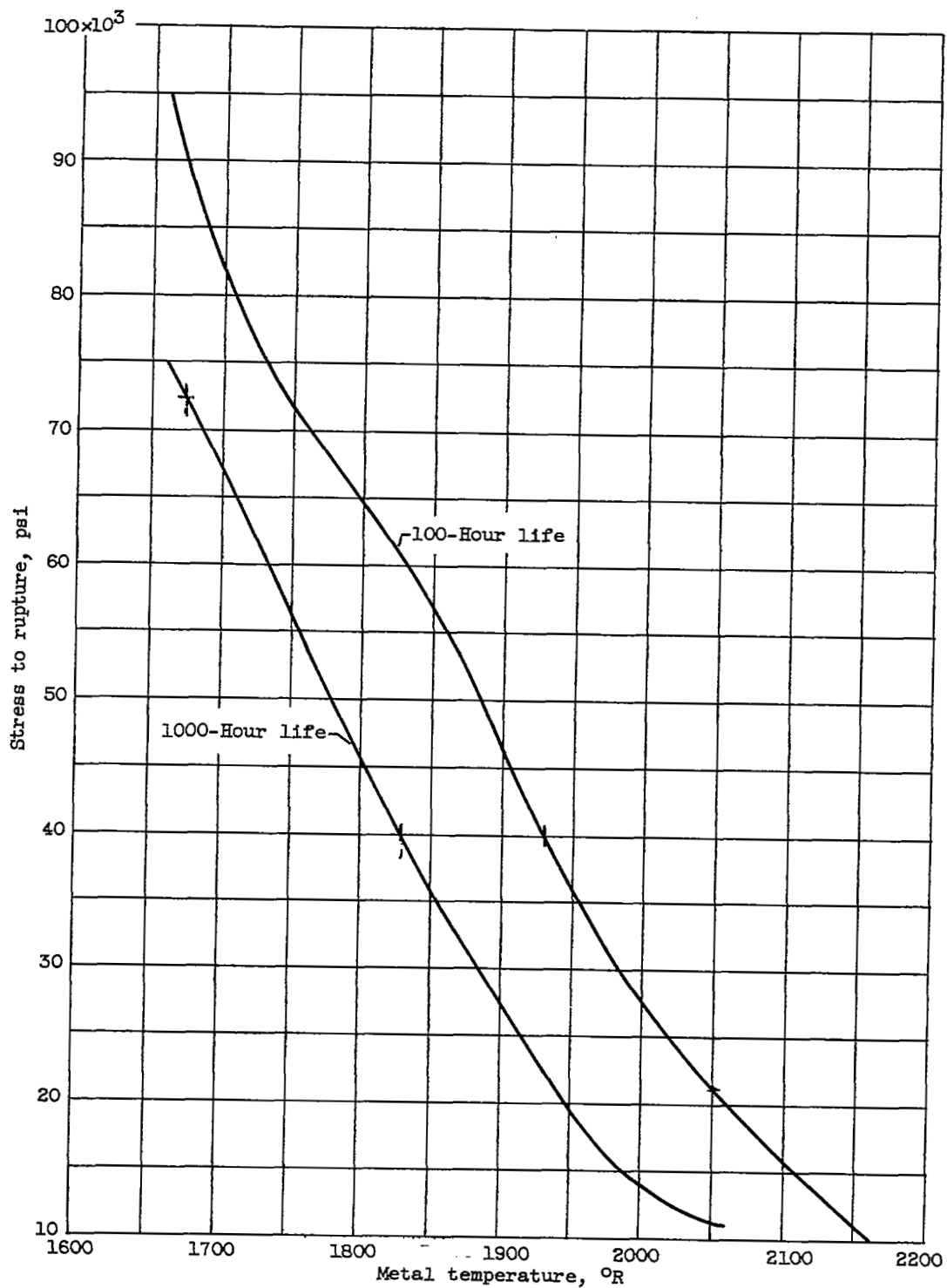


Figure 1. - Rupture stress for metal M-252.

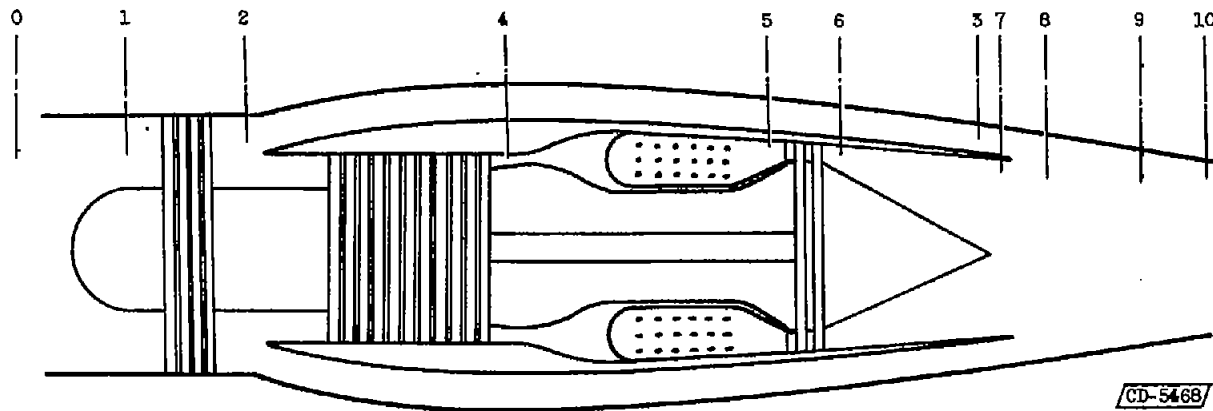
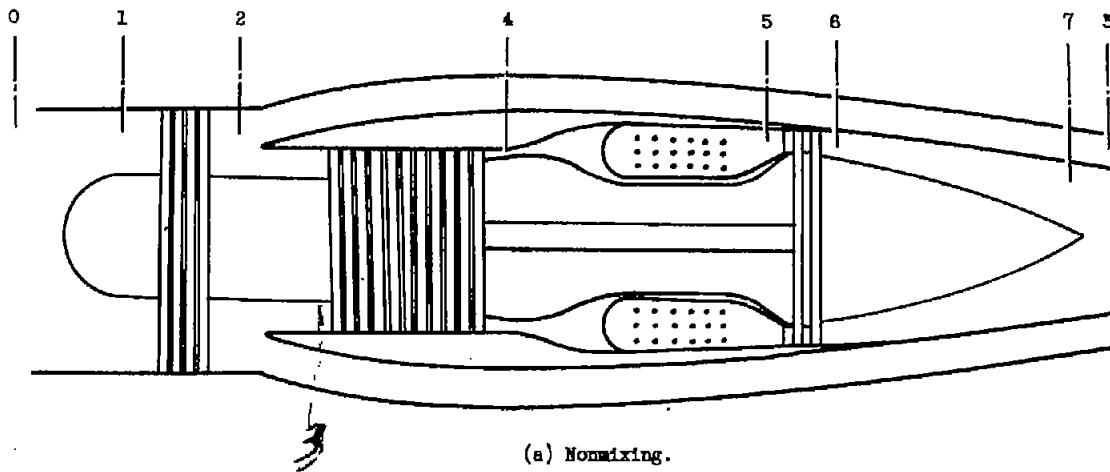


Figure 2. - Schematic sketch of ducted-fan engine.

CD-5468

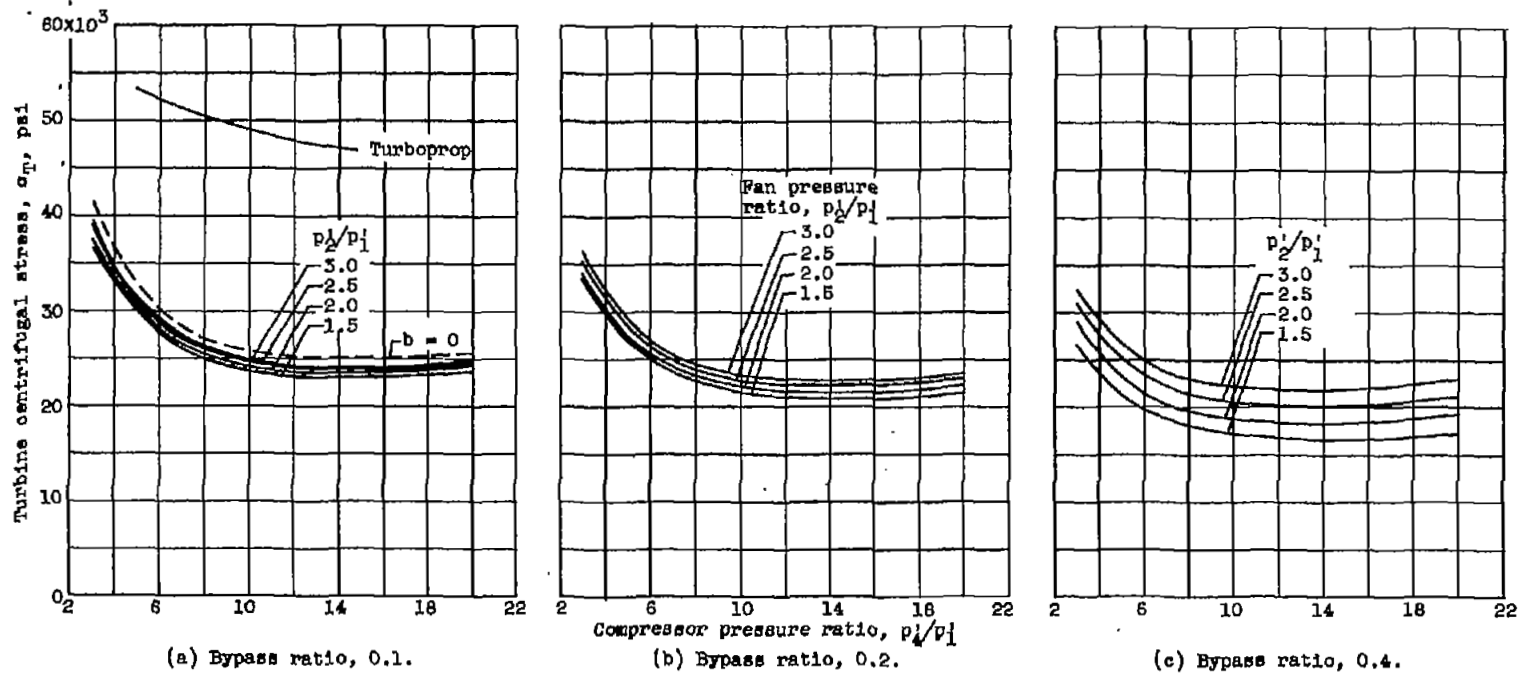
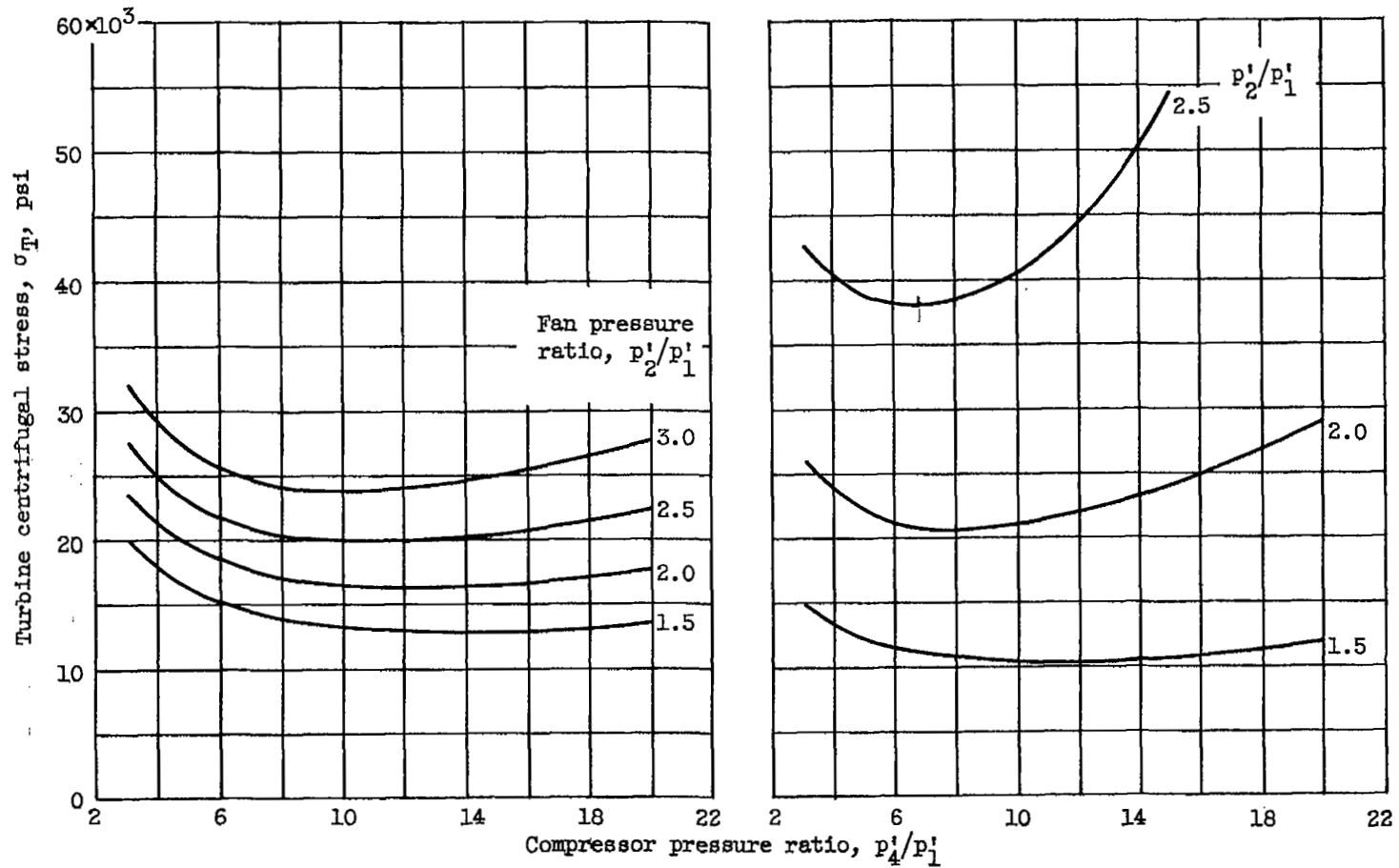


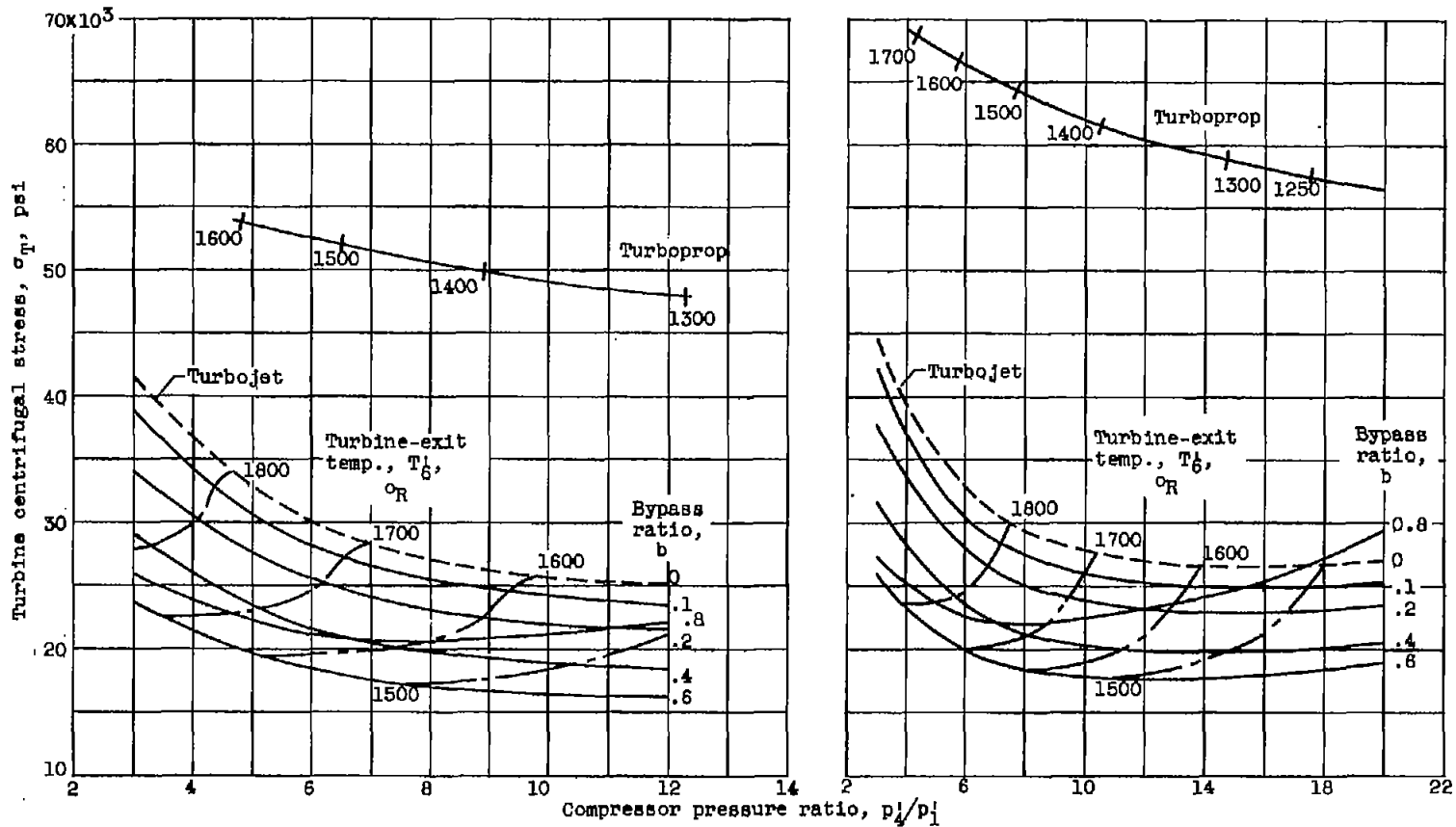
Figure 3. - Effects of compressor pressure ratio, bypass ratio, and fan pressure ratio on turbine stress for sea-level static designs at turbine-inlet temperature of 2075°R . Parameter e_F , 44×10^6 pounds/second⁵.



(d) Bypass ratio, 0.6.

(e) Bypass ratio, 0.8.

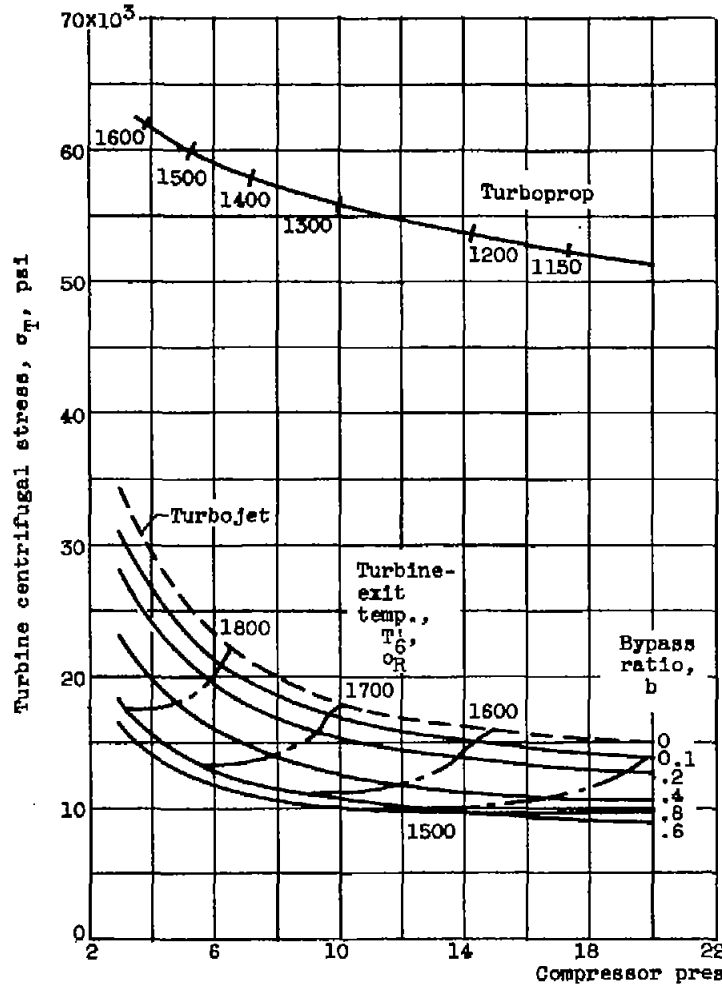
Figure 3. - Concluded. Effects of compressor pressure ratio, bypass ratio, and fan pressure ratio on turbine stress for sea-level static designs at turbine-inlet temperature of 2075° R. Parameter e_p , 44×10^6 pounds/second³.



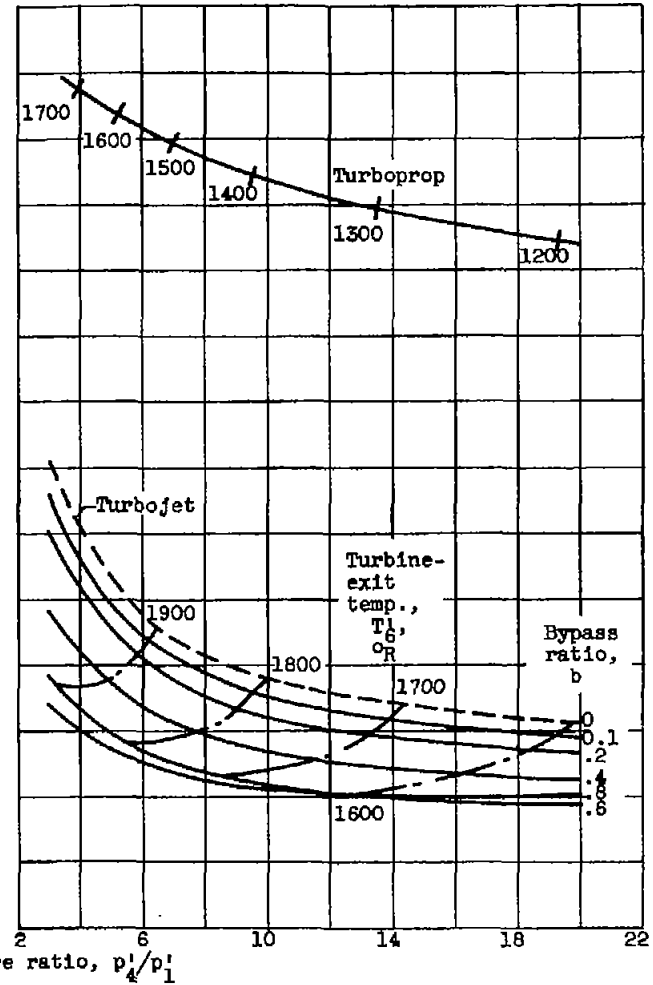
(a) Sea-level static designs at 2075° R.

(b) Sea-level Mach 0.6 designs at 2225° R.

Figure 4. - Effects of compressor pressure ratio, bypass ratio, and flight Mach number on turbine stress. Parameter c_p , 44×10^6 pounds/second³; fan pressure ratio, 2.0.

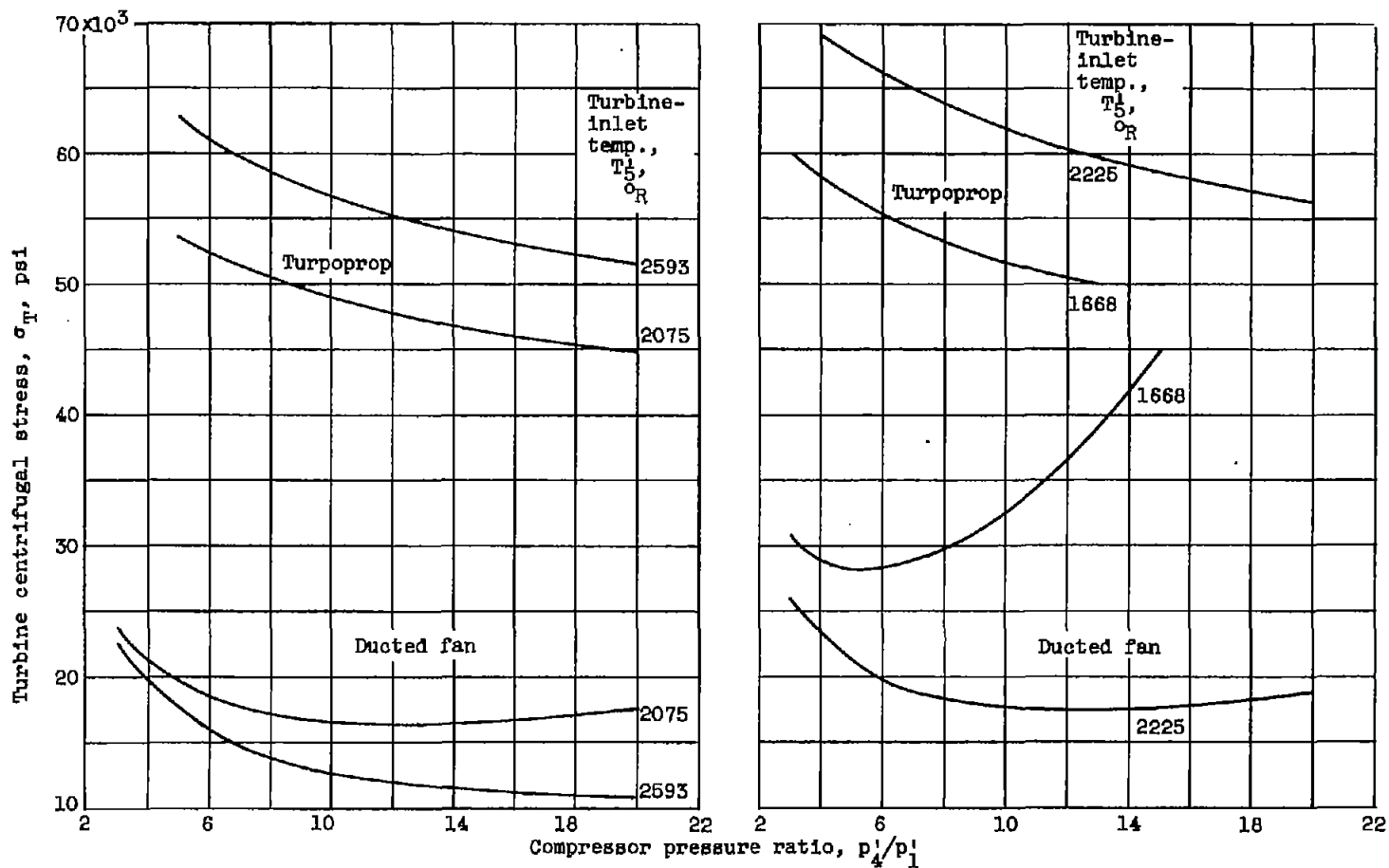


(c) Tropopause Mach 0.6 designs at 2090° R.



(d) Tropopause Mach 0.8 designs at 2200° R.

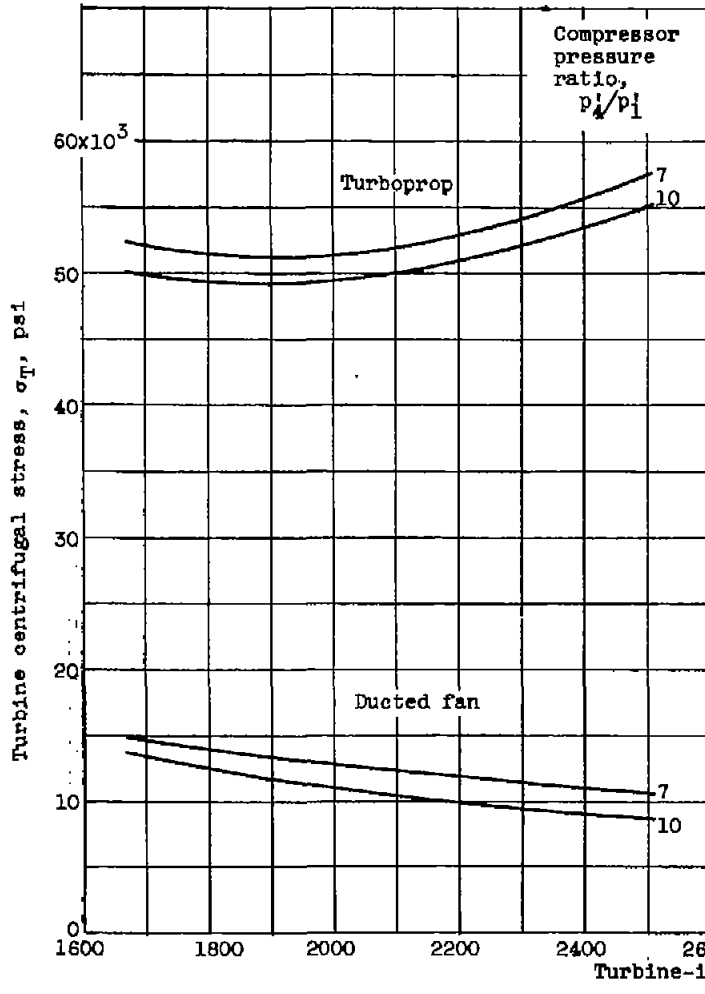
Figure 4. - Concluded. Effects of compressor pressure ratio, bypass ratio, and flight Mach number on turbine stress. Parameter e_p , 44×10^6 pounds/second³; fan pressure ratio, 2.0.



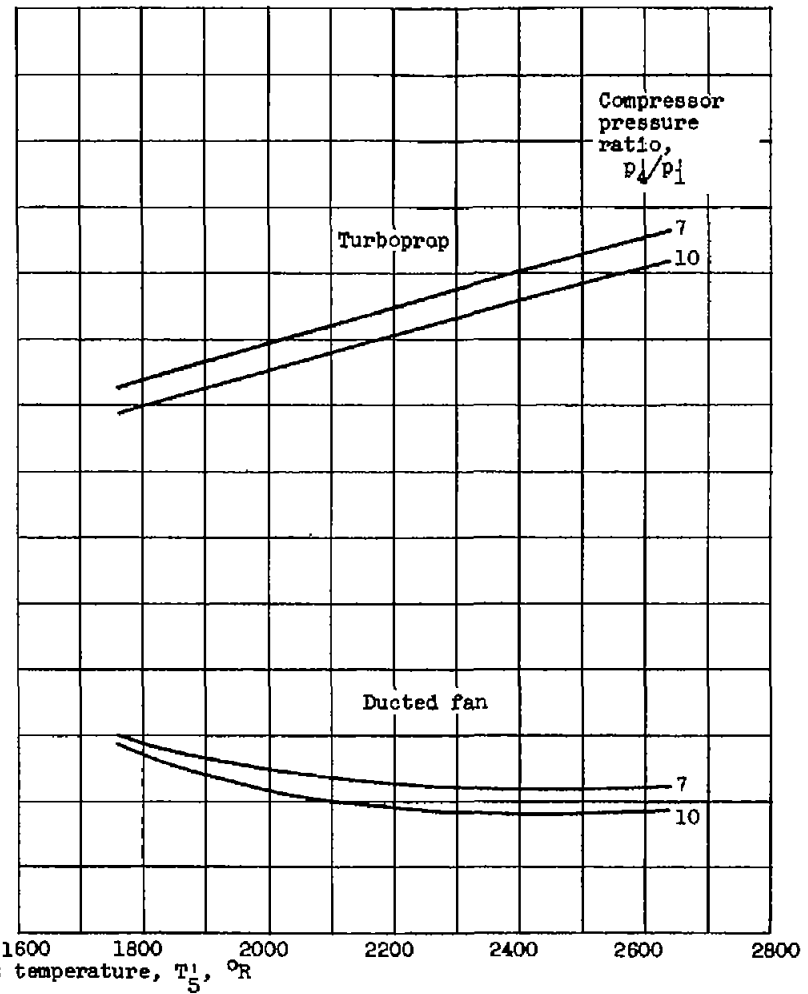
(a) Sea-level static designs.

(b) Sea-level Mach 0.6 designs.

Figure 5. - Effects of turbine-inlet temperature, compressor pressure ratio, and flight Mach number on turbine stress. Parameter e_p , 44×10^8 pounds/second³; fan pressure ratio, 2.0; bypass ratio, 0.6.

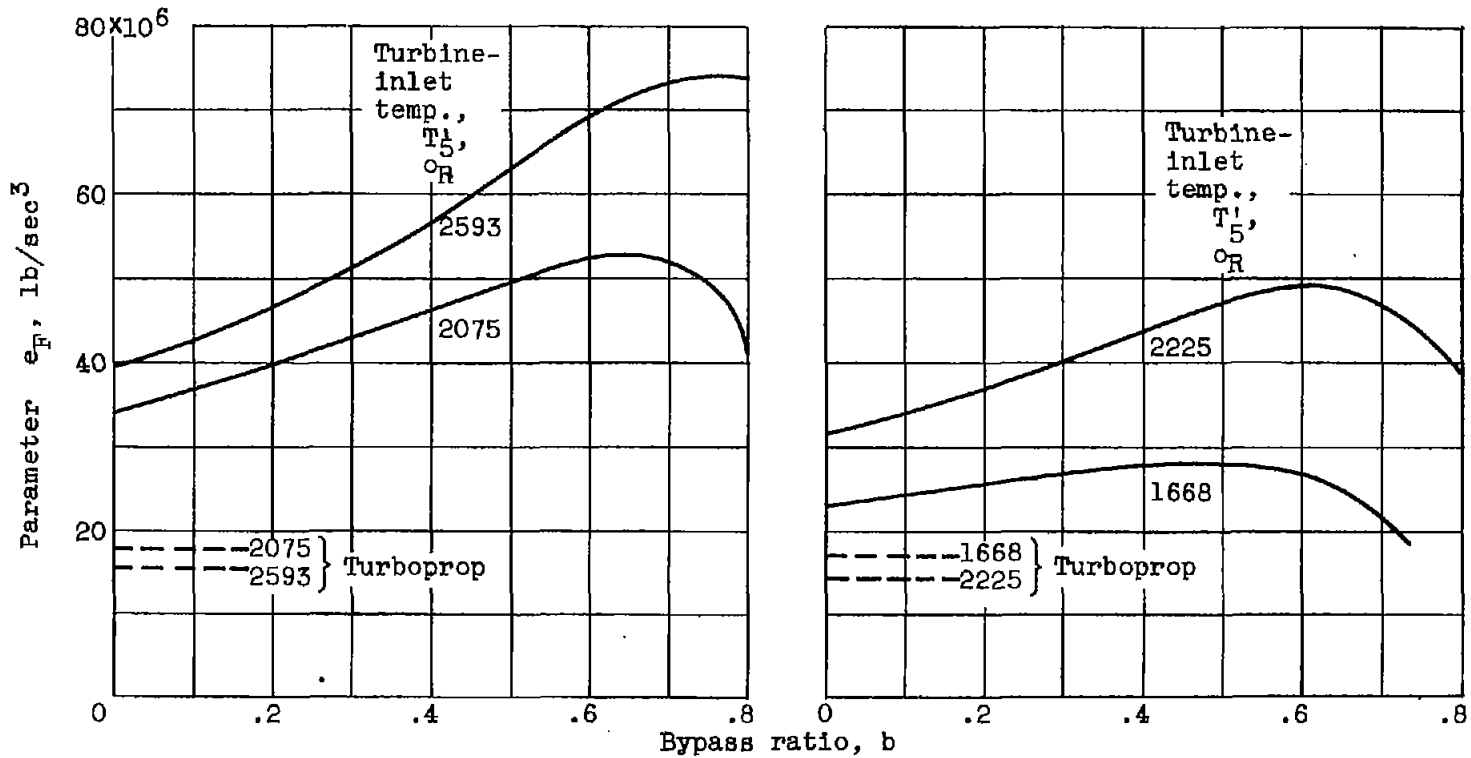


(c) Tropopause Mach 0.6 designs.



(d) Tropopause Mach 0.8 designs.

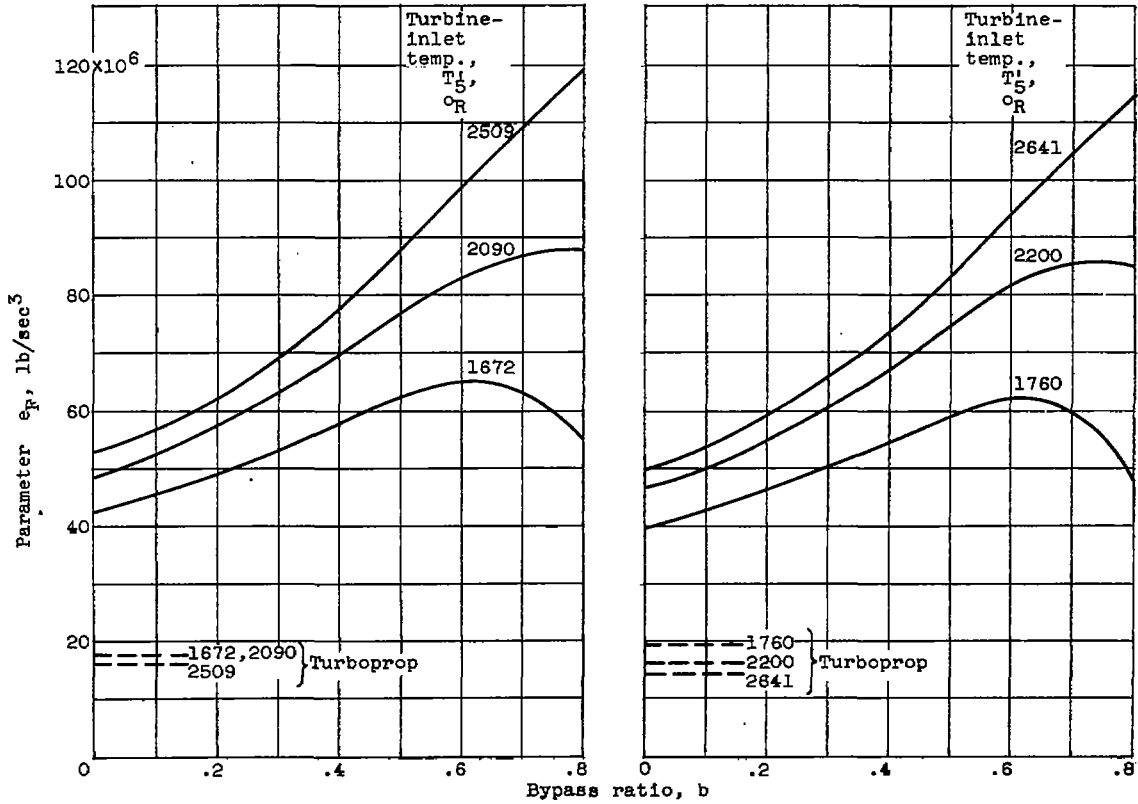
Figure 5. - Concluded. Effects of turbine-inlet temperature, compressor pressure ratio, and flight Mach number on turbine stress. Parameter e_p , 44×10^8 pounds/second³; fan pressure ratio, 2.0; bypass ratio, 0.6.



(a) Sea-level static designs.

(b) Sea-level Mach 0.6 designs.

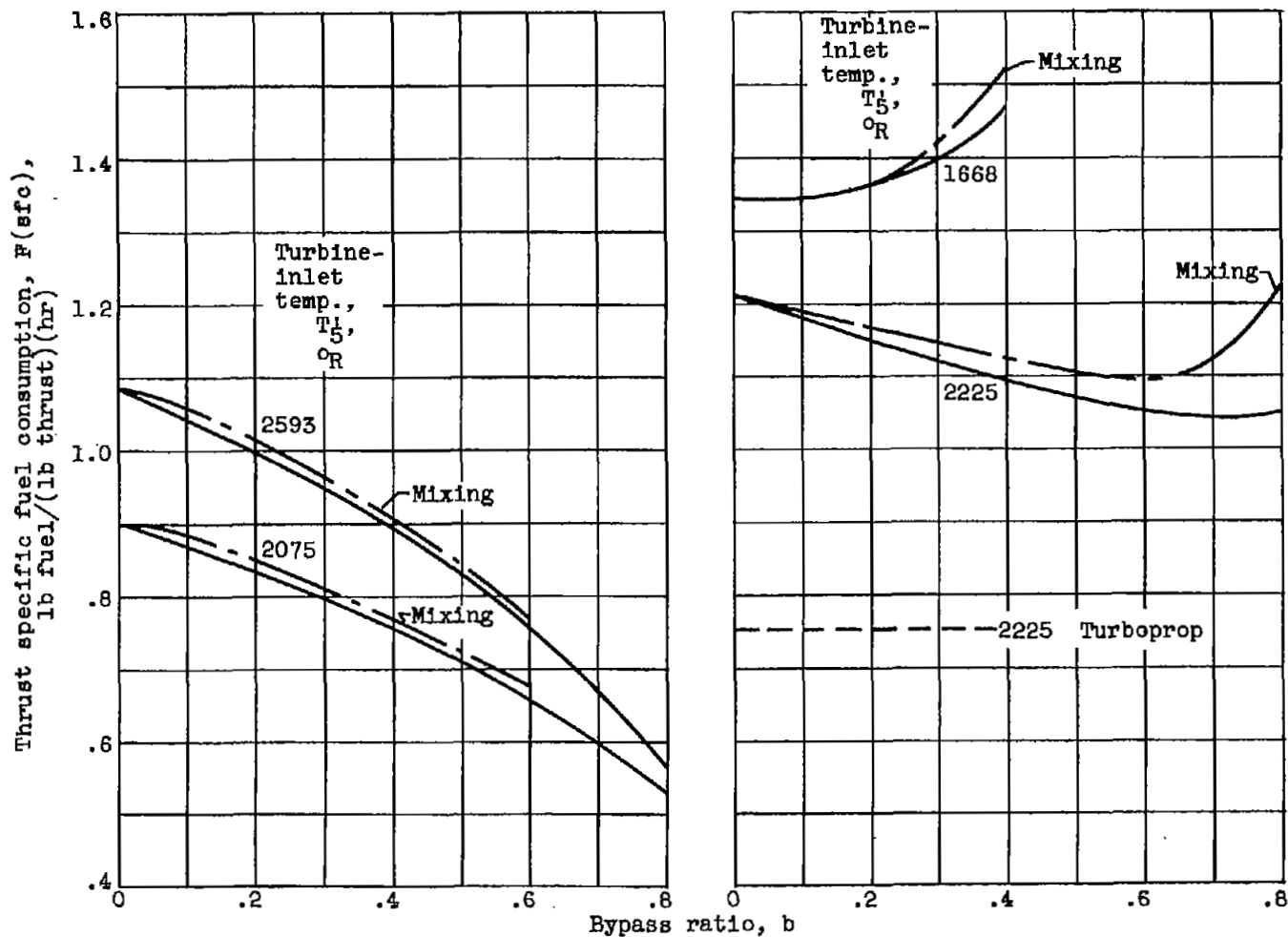
Figure 6. - Effects of bypass ratio, turbine-inlet temperature, and flight Mach number on parameter e_F . Turbine stress, 20,000 psi; compressor pressure ratio, 10; fan pressure ratio, 2.0.



(c) Tropopause Mach 0.6 designs.

(d) Tropopause Mach 0.8 designs.

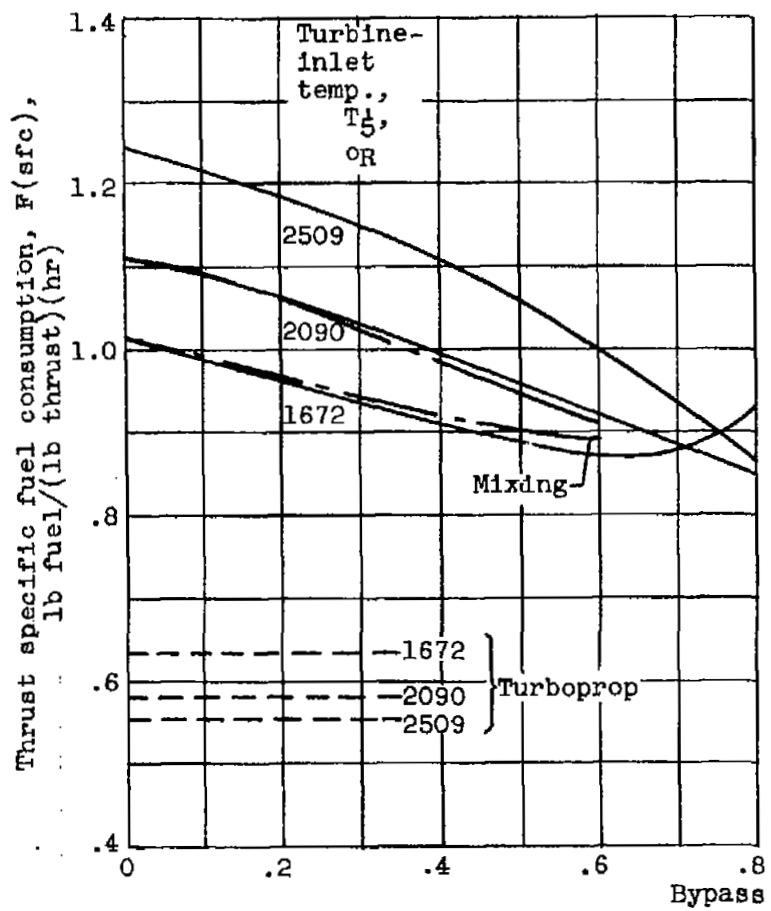
Figure 6. - Concluded. Effects of bypass ratio, turbine-inlet temperature, and flight Mach number on parameter e_p . Turbine stress, 20,000 psi; compressor pressure ratio, 10; fan pressure ratio, 2.0.



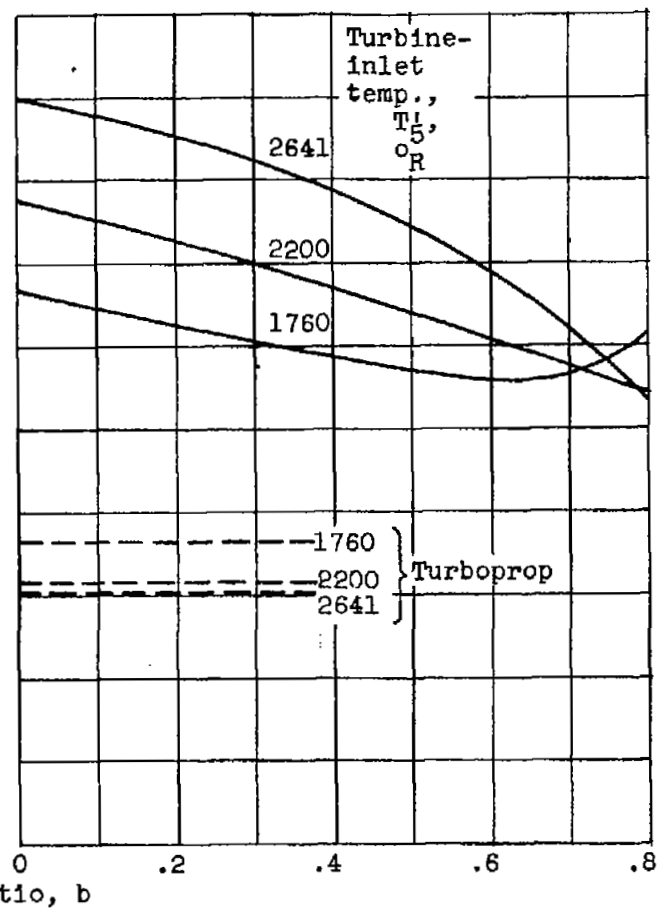
(a) Sea-level static designs.

(b) Sea-level Mach 0.6 designs.

Figure 7. - Effects of bypass ratio, mixing, turbine-inlet temperature, and flight Mach number on minimum thrust specific fuel consumption. Compressor pressure ratio, 10.



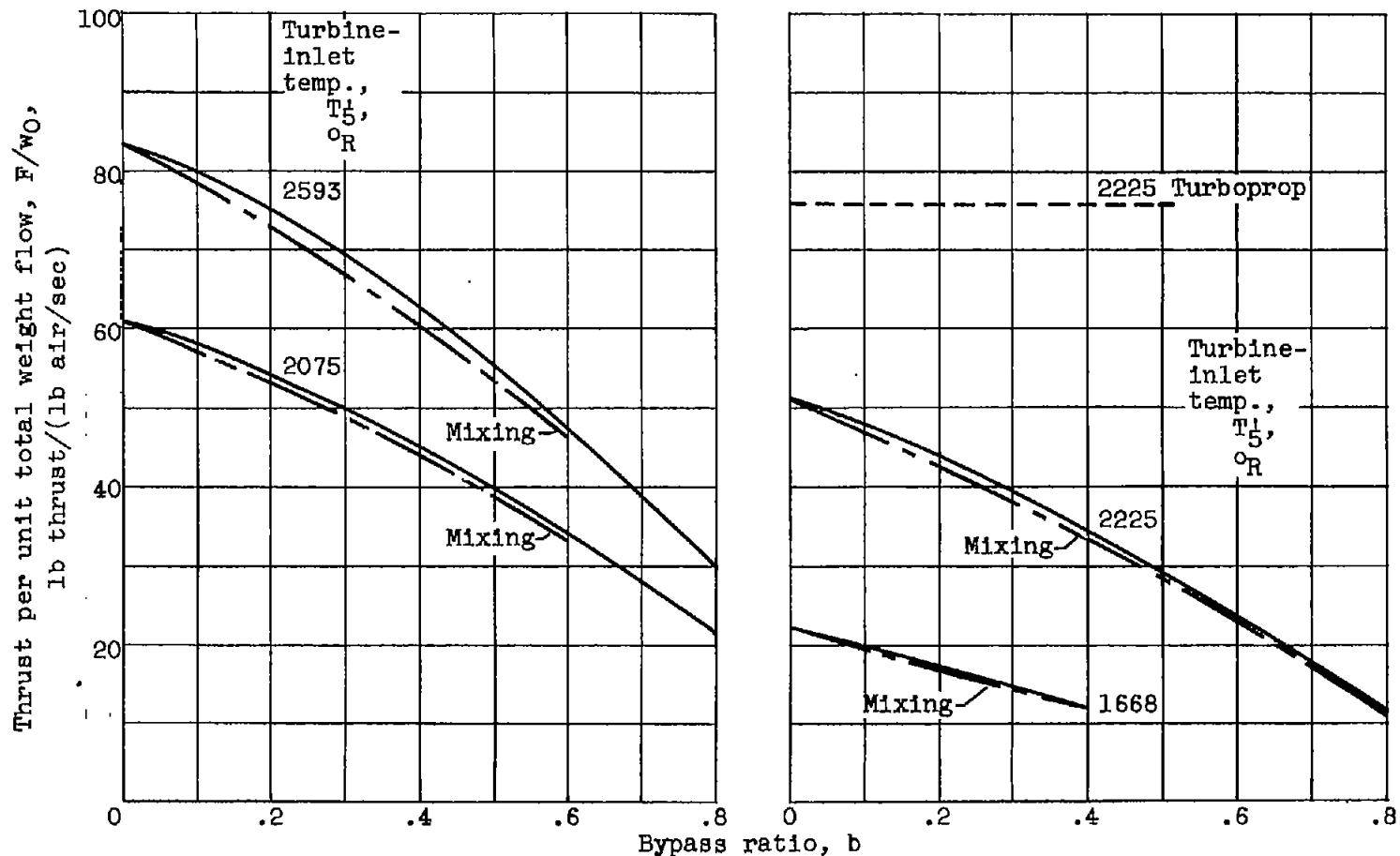
(c) Tropopause Mach 0.6 designs.



(d) Tropopause Mach 0.8 designs.

Figure 7. - Concluded. Effects of bypass ratio, mixing, turbine-inlet temperature, and flight Mach number on minimum thrust specific fuel consumption. Compressor pressure ratio, 10.

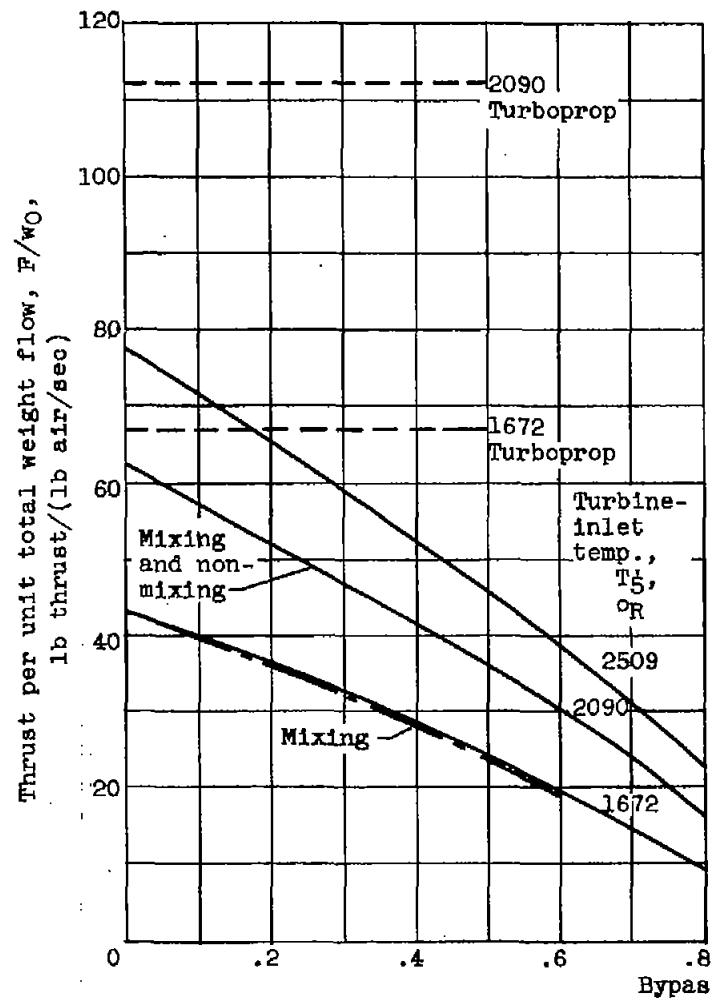
1037



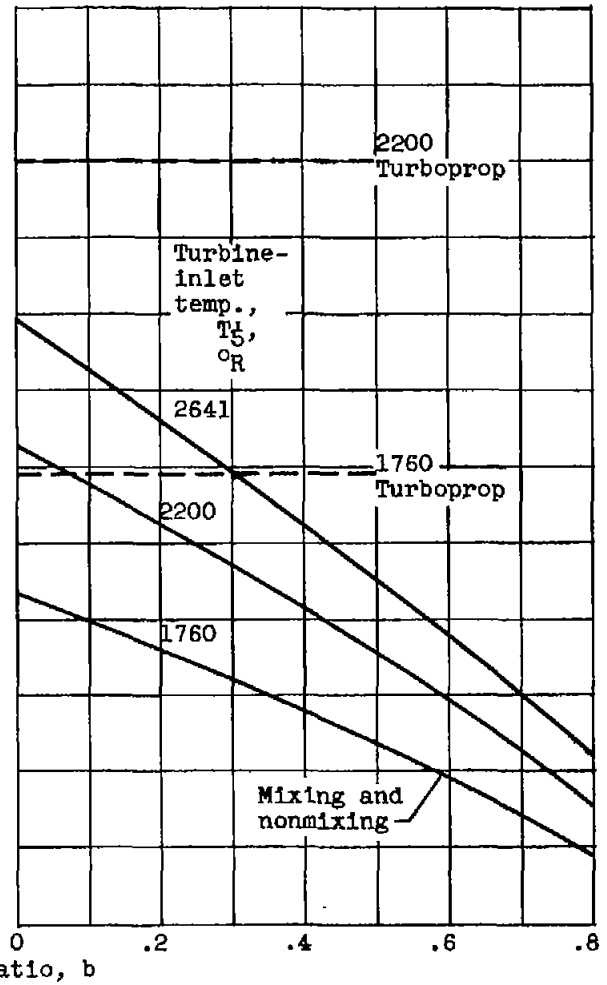
(a) Sea-level static designs.

(b) Sea-level Mach 0.6 designs.

Figure 8. - Effects of bypass ratio, mixing, turbine-inlet temperature, and flight Mach number on thrust per unit total weight flow for minimum thrust specific fuel consumption. Compressor pressure ratio, 10.

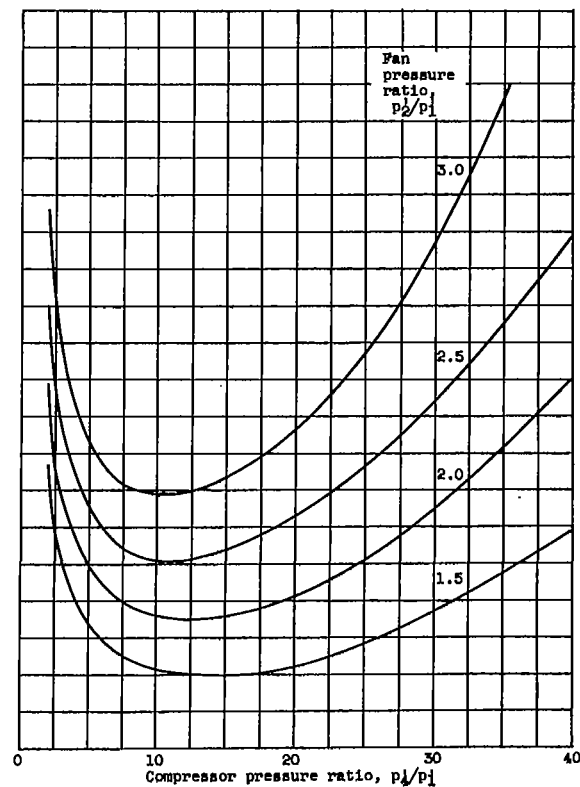
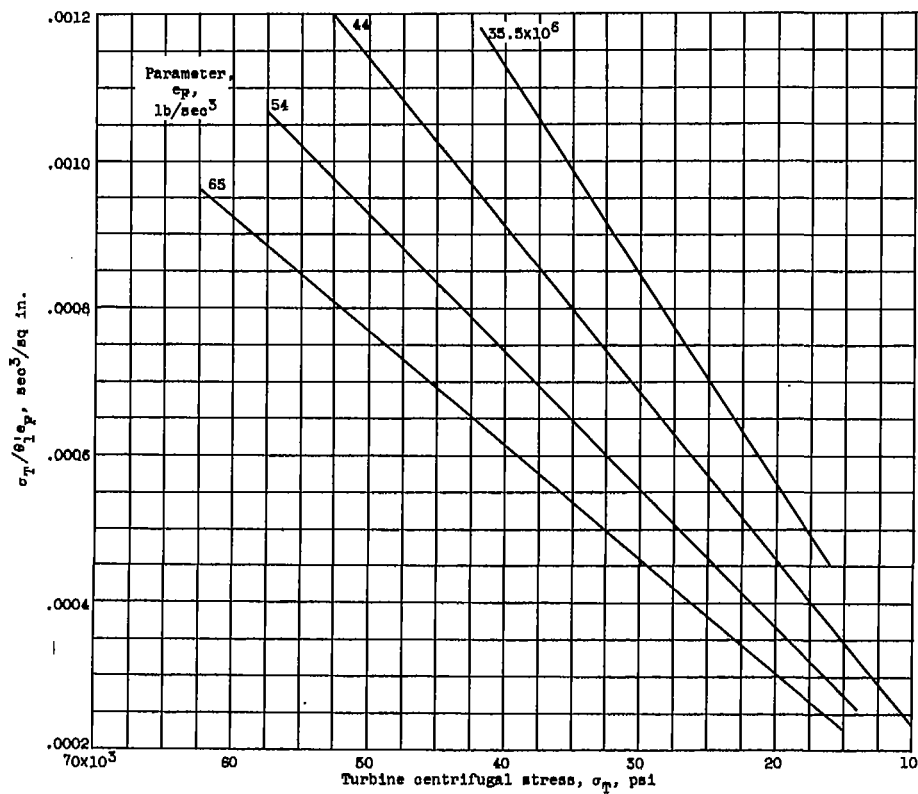


(c) Tropopause Mach 0.6 designs.



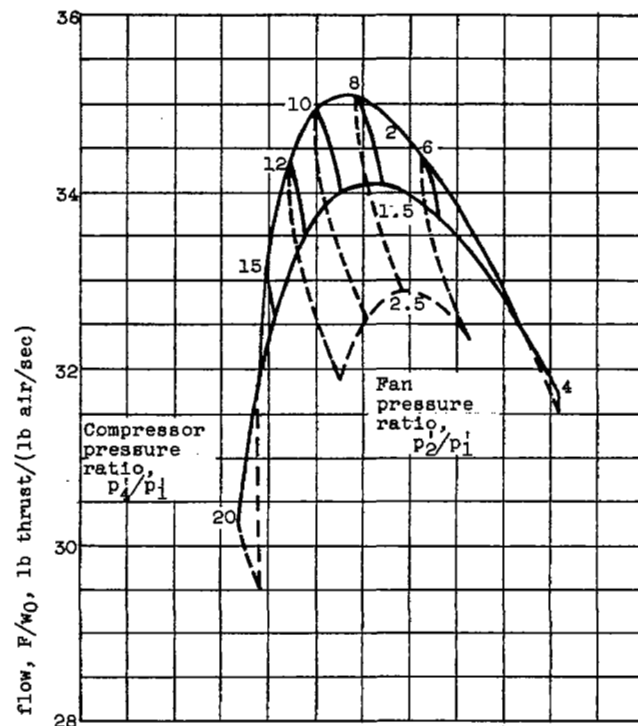
(d) Tropopause Mach 0.8 designs.

Figure 8. - Concluded. Effects of bypass ratio, mixing, turbine-inlet temperature, and flight Mach number on thrust per unit total weight flow for minimum thrust specific fuel consumption. Compressor pressure ratio, 10.

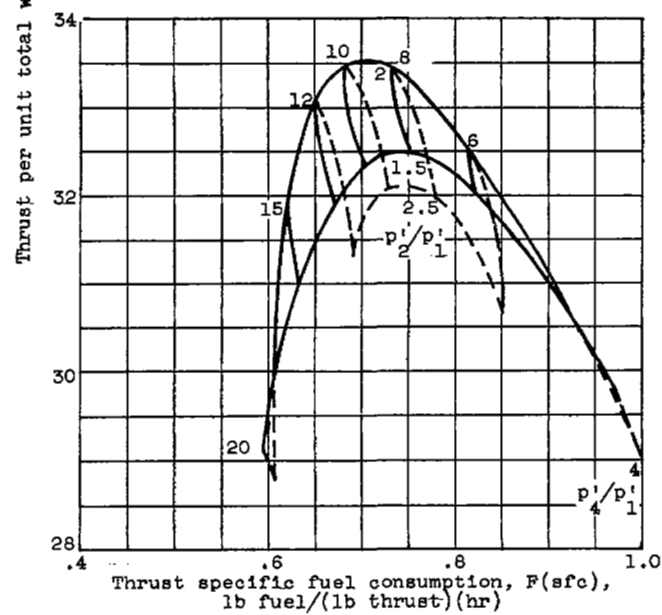


(a) Engine parameters.

Chart I. - Ducted-fan-engine performance. Flight Mach number at sea level, 0; turbine-inlet temperature, 2075° R; engine temperature ratio, 4; bypass ratio, 0.6.

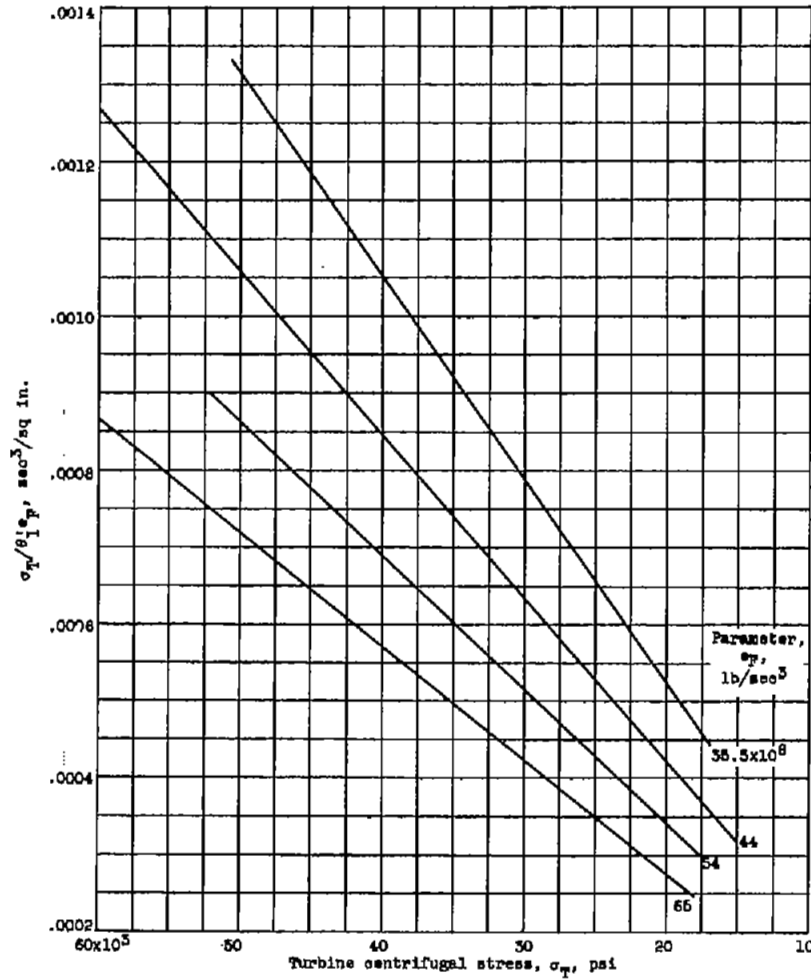


(b) Performance parameters without mixing.



(c) Performance parameters with mixing.

Chart I. - Concluded. Ducted-fan-engine performance. Flight Mach number at sea level, 0; turbine-inlet temperature, $2075^{\circ}R$; engine temperature ratio, 4; bypass ratio, 0.6.



(a) Engine parameters.

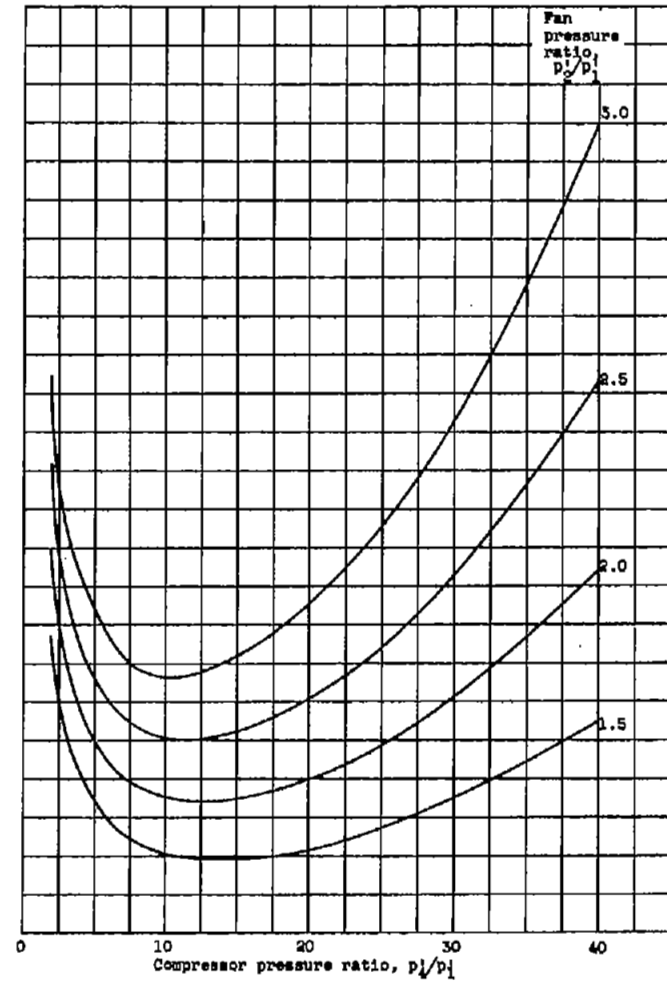
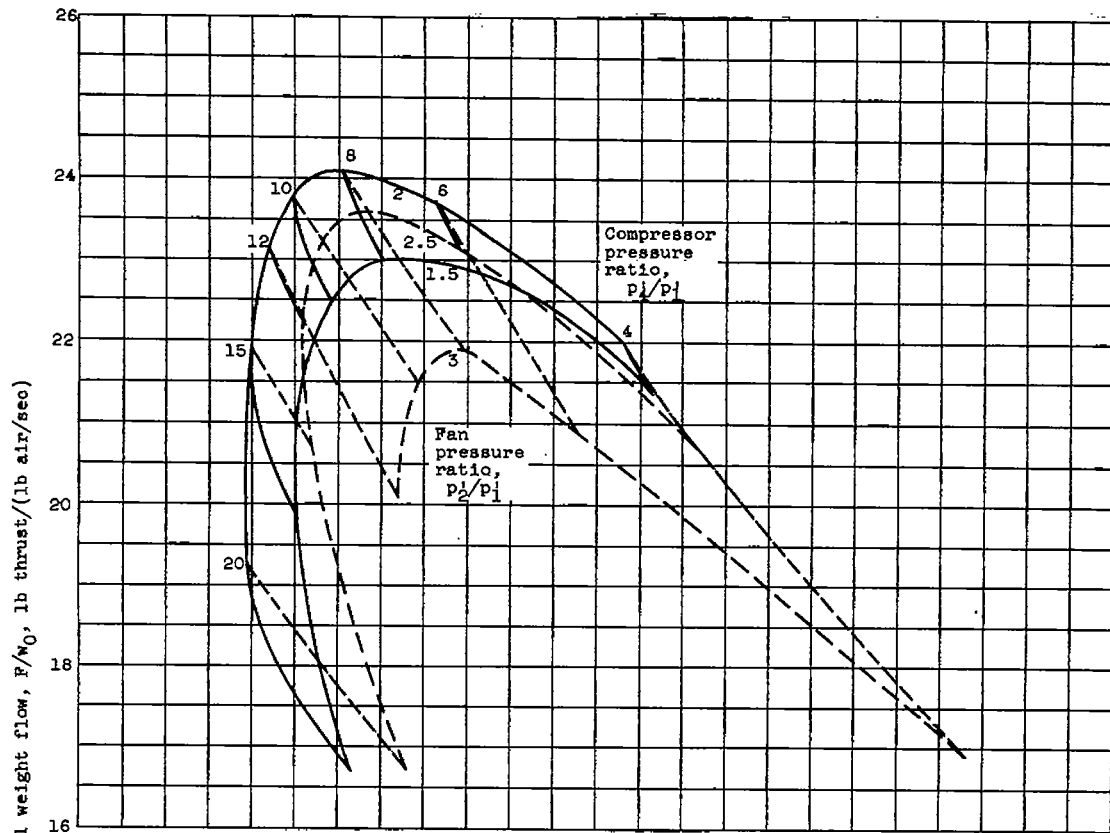
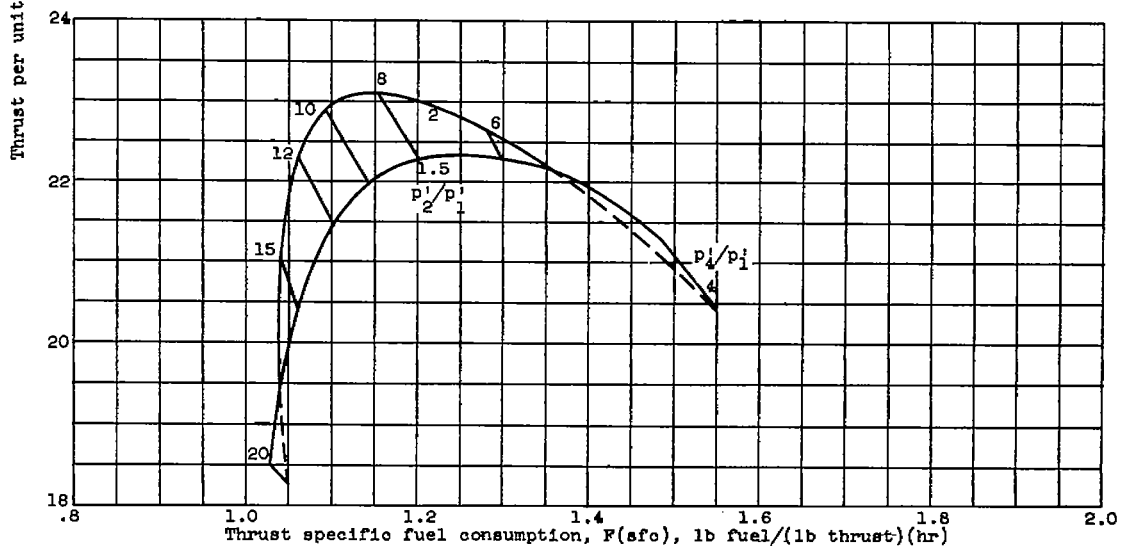


Chart II. - Ducted-fan-engine performance. Flight Mach number at sea level, 0.6; turbine-inlet temperature, 2225° R; engine temperature ratio, 4; bypass ratio, 0.6.

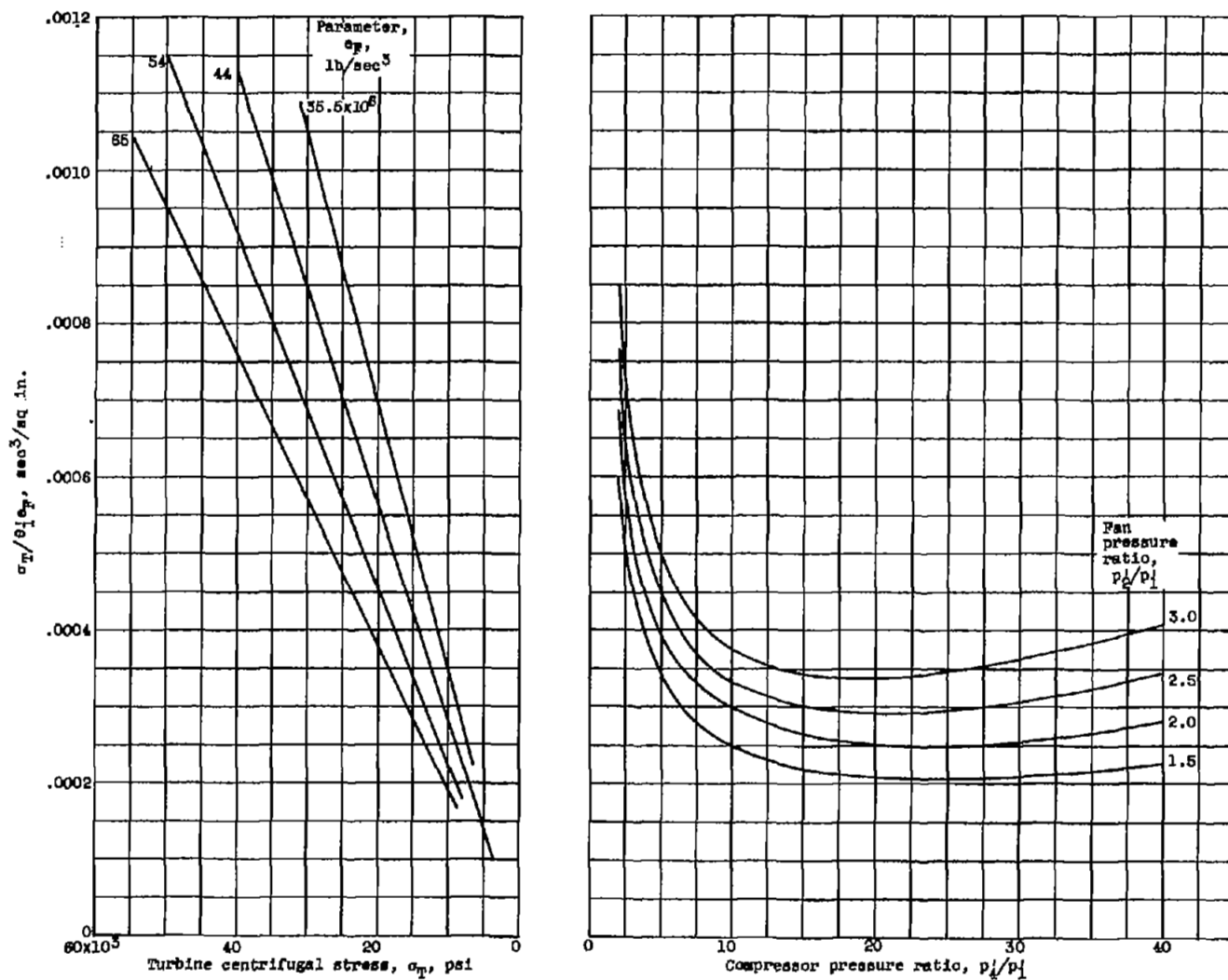


(b) Performance parameters without mixing.



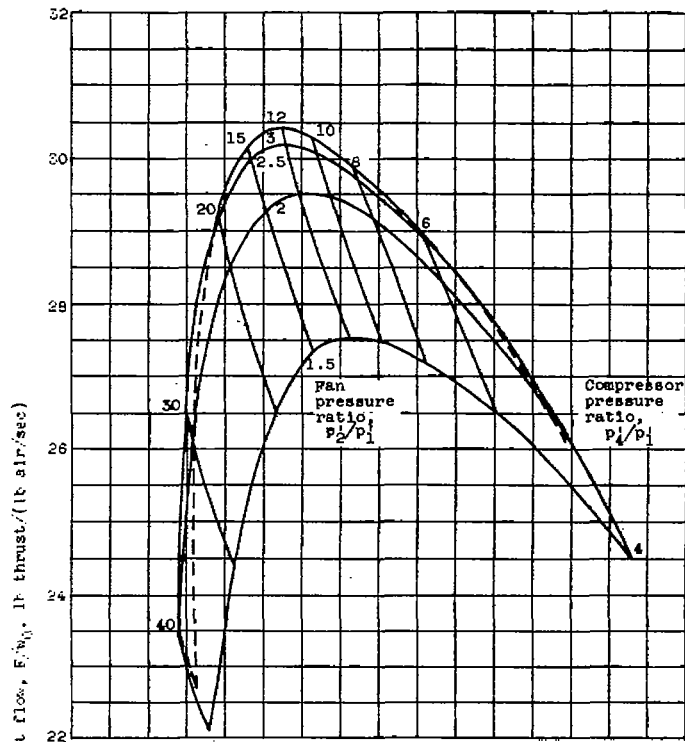
(c) Performance parameters with mixing.

Chart II. - Concluded. Ducted-fan-engine performance. Flight Mach number at sea level, 0.6; turbine-inlet temperature, 2225° R; engine temperature ratio, 4; bypass ratio, 0.6.

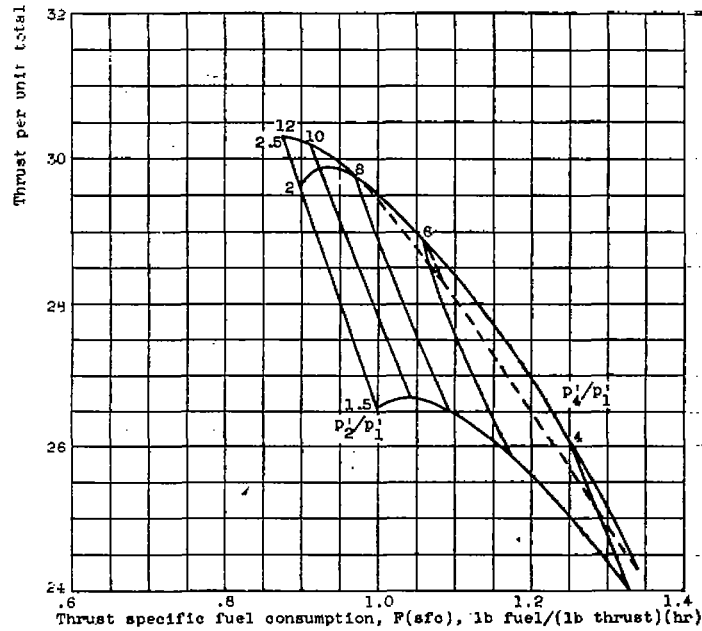


(a) Engine parameters.

Chart III. - Ducted-fan-engine performance. Flight Mach number at tropopause, 0.6; turbine-inlet temperature, 2090° R; engine temperature ratio, S; bypass ratio, 0.6.

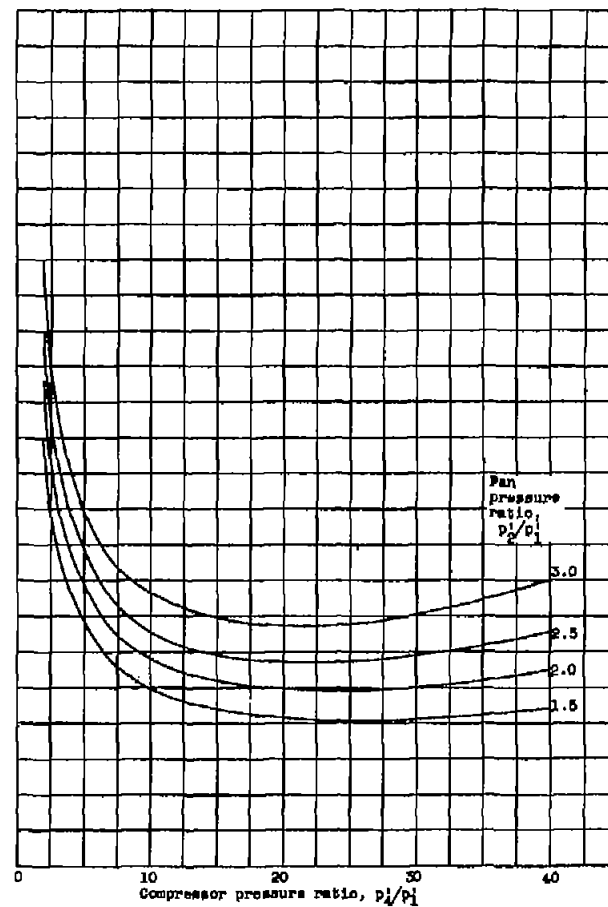
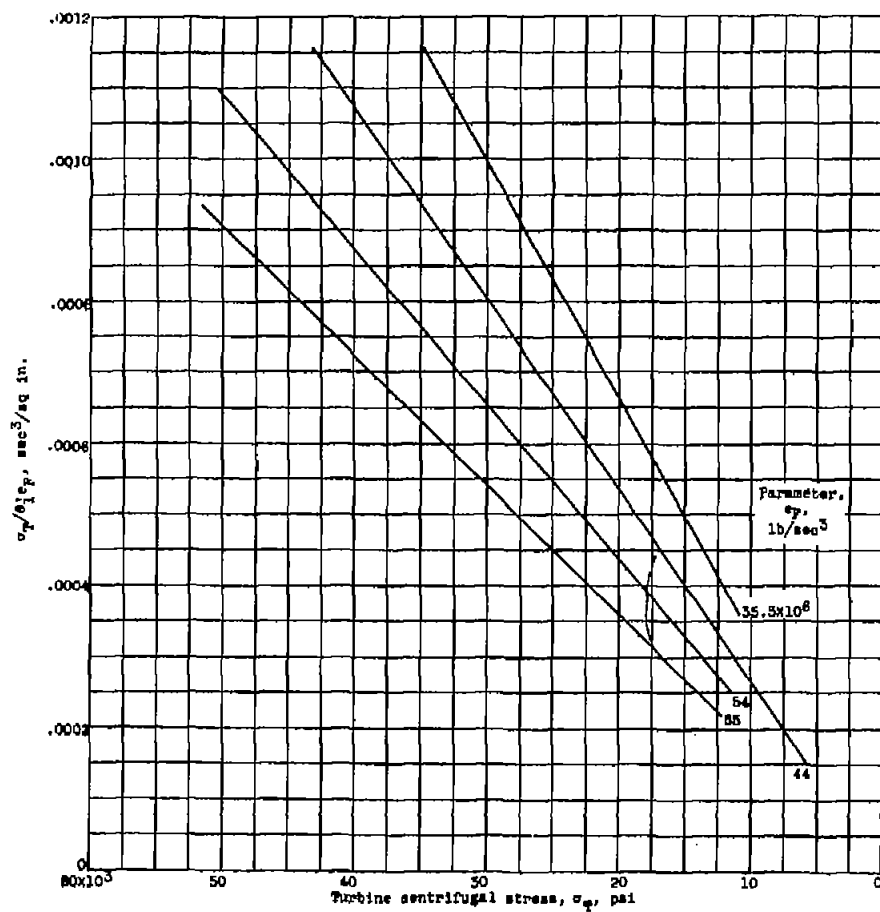


(b) Performance parameters without mixing.



(c) Performance parameters with mixing.

Chart III. - Concluded. Ducted-fan-engine performance. Flight Mach number at tropopause, 0.6; turbine-inlet temperature, 2090° R; engine temperature ratio, 5; bypass ratio, 0.6.



(a) Engine parameters.

Chart IV. - Ducted-fan-engine performance. Flight Mach number at tropopause, 0.8; turbine-inlet temperature, 2200°R ; engine temperature ratio, 5; bypass ratio, 0.6.

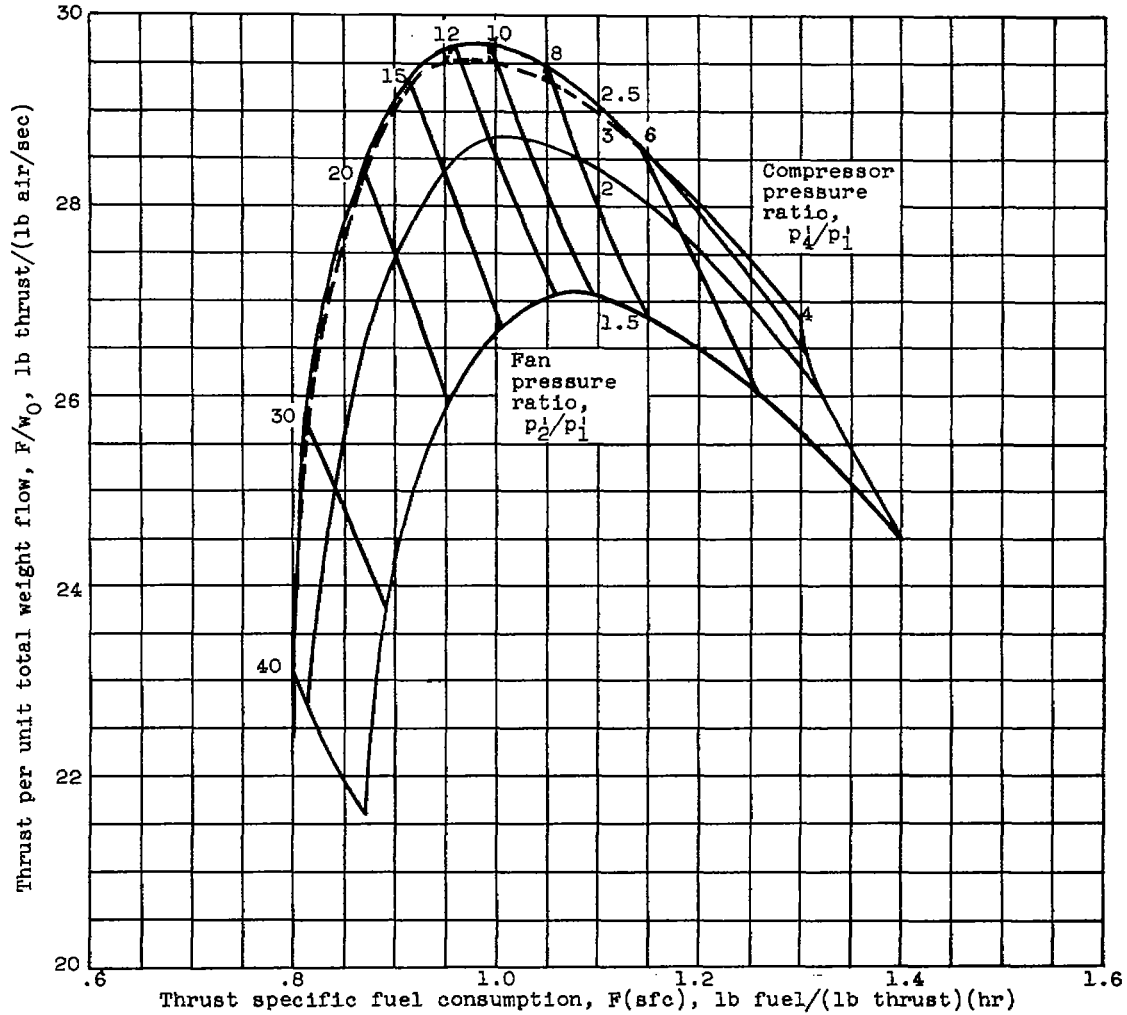
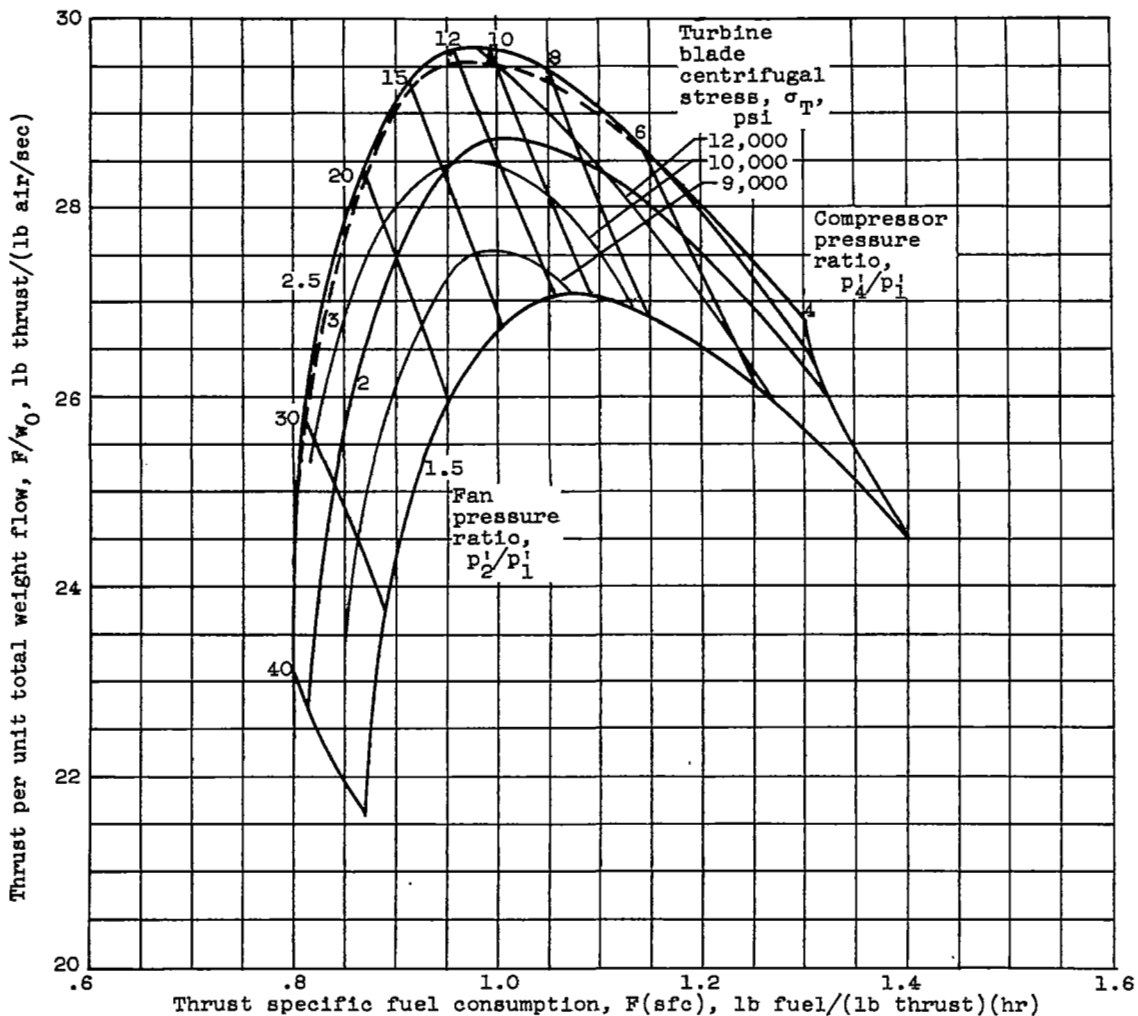


Chart IV. - Continued. Ducted-fan-engine performance. Flight Mach number at tropopause, 0.8; turbine-inlet temperature, 2200° R; engine temperature ratio, 5; bypass ratio, 0.6.

4307



(c) Performance parameters without mixing. Lines of constant stress for $e_F = 44 \times 10^6$ pounds/second³.

Chart IV. - Concluded. Ducted-fan-engine performance. Flight Mach number at tropopause, 0.8; turbine-inlet temperature, 2200° R; engine temperature ratio, 5; bypass ratio, 0.6.

NASA Technical Library



3 1176 01436 5903

